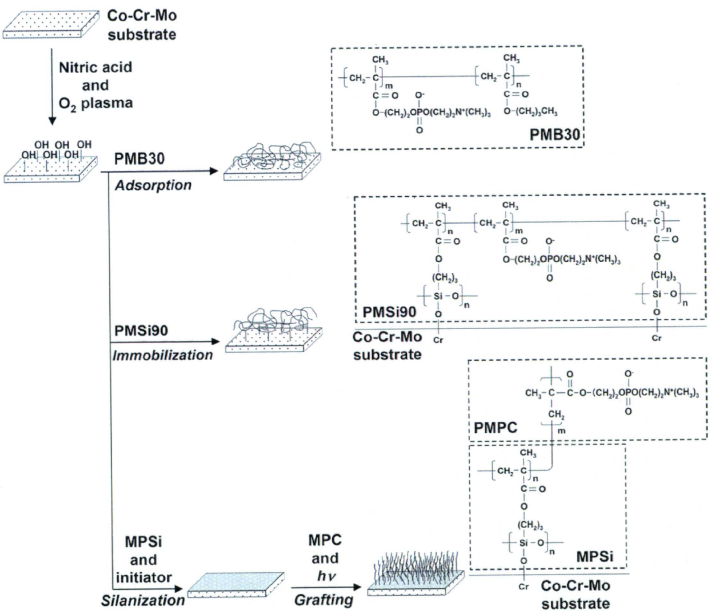

Fig. 1. Schematic illustration for the preparation of MPC polymer-coated and PMPC-grafted Co–Cr–Mo.

2.7. Cross-sectional observation by transmission electron microscopy

A cross-section of the surface-modified Co–Cr–Mo samples was observed using a transmission electron microscope (TEM) and by energy dispersive X-ray (EDX) spectroscopy. The specimens were precoated with an aluminum film; then, a thin film of the samples was prepared by the focused ion beam (FIB) technique using an FB-2000A (Hitachi High-Technologies Co., Tokyo, Japan) FIB system. The samples were thinned to electron transparency by a low gallium ion beam current. The thin film thus prepared was positioned onto a copper TEM mesh grid. TEM observations were then recorded using an HF-2000 electron microscope (Hitachi High-Technologies Co.) at an acceleration voltage of 200 kV. EDX spectra were analyzed on a cross-section of the samples using a Sigma EDX attachment (Kevex Instruments, Inc., Valencia, CA, USA) at an acceleration voltage of 200 kV.

2.8. Characterization of protein adsorption by micro bicinchoninic acid method

The amounts of protein adsorbed on the surface-modified Co–Cr–Mo samples were determined by the micro bicinchoninic acid (BCA) method. Each specimen was immersed in PBS for 1 h to equilibrate the surface modified by the MPC polymer. The specimens were immersed in bovine serum albumin (BSA, $Mw = 6.7 \times 10^4$; Sigma–Aldrich Corp., MO, USA), bovine blood γ-globulins ($Mw = 1.5 \times 10^5$; Sigma–Aldrich Co.), and bovine plasma fibrinogen ($Mw = 3.4 \times 10^5$; Sigma–Aldrich Co.) solutions at 37 °C for 1 h. The protein solutions were prepared in BSA, γ-globulins, and fibrinogen concentrations of 4.5, 1.6, and 0.3 g/L, respectively, i.e., 10% of the concentration of human plasma levels. Then, the specimens were rinsed five times with fresh PBS and immersed in 1 mass% sodium dodecyl sulfate (SDS) aqueous solution and shaken at room temperature for 1 h to completely detach the adsorbed BSA, γ-globulins, and fibrinogen on the surface modified by the MPC polymer. A protein analysis kit (micro BCA protein assay kit, #23235; Thermo Fisher Scientific Inc., IL, USA) based on the BCA method was used to determine the BSA concentration in the SDS solution, and the amount of BSA, γ-globulins, and fibrinogen adsorbed on the surface modified by the MPC polymer was calculated.

2.9. Friction test and histological observation of articular cartilage

The coefficients of dynamic friction between the pins fabricated from articular cartilage and the surface-modified Co–Cr–Mo plates were measured by using a pin-on-plate machine (Tribostation 32; Shinto Scientific Co., Ltd., Tokyo, Japan). The friction tests were performed at room temperature and 37 °C with various loads in the range from 0.49 to 9.80 N, sliding distance of 25 mm, and frequency of 1 Hz for a maximum of 5×10^3 cycles [21]. Pure water, mixture of 25 vol% bovine serum (BS), 20 mM/L of ethylene diamine tetraacetic acid (EDTA), 0.1 mass% sodium azide, and the BS mixture containing 0.02 mass% MPC polymer (PMB30 ($Mw = 5.0 \times 10^4$), PMSi90 ($Mw = 9.8 \times 10^4$), and PMPC ($Mw = 1.0 \times 10^5$)) were used as a lubricant each. Subsequently, five replicate measurements were performed for each sample, and the average values were regarded as the coefficients of dynamic friction. After 100 cycles of friction tests, the plate samples were FM-observed. Then, after 5×10^3 cycles friction test, articular cartilage pins against the untreated Co–Cr–Mo and PMPC-grafted Co–Cr–Mo were fixed with 10% neutral buffered formalin for 3 d, then decalcified in KC-X solution (Falma Co., Tokyo, Japan) for 8 d, and then dehydrated in graded ethanol for histological observation. The decalcified cartilage specimens were embedded in paraffin (Tissue-prep; Fisher Scientific Corp., Fair Lawn, NJ, USA), and microsections were prepared and stained with hematoxylin (Real hematoxylin; Dako Co., Carpinteria, CA, USA) and eosin (Eosin yellowish; Kanto Chemical Co., Inc.) (H&E) as well as with Safranin O (Nacalai Tesque, Inc., Kyoto, Japan) and observed with a microscope (Eclipse E600; Nikon Corp., Tokyo, Japan) equipped with a CCD camera (DP72; Olympus Co., Tokyo, Japan).

2.10. PBS soaking test

The surface-modified Co–Cr–Mo samples ($10 \times 10 \times 1$ mm^3 in size) were soaked in 50 mL of PBS. After soaking with 120 rpm shaking at 37 °C for 1, 4, 8, and 12 weeks, the samples removed from the PBS and were characterized by XPS analysis, water-contact angle measurement, and FM observation.

Table 1
Surface elemental composition ($n = 5$) and static-water contact angle ($n = 15$) of untreated, MPC polymer-coated and PMPC-grafted Co–Cr–Mo alloy.

Sample	Surface elemental composition (atom%)								Contact angle (deg)
	C_{1s}	O_{1s}	N_{1s}	P_{2p}	Si_{2p}	Co_{2p}	Cr_{2p}	Mo_{3d}	
Co–Cr–Mo (untreated)	14.6 (1.3)[a]	52.9 (2.7)	0.0 (0.0)	0.0 (0.0)	0.0 (0.0)	26.7 (1.5)	5.4 (0.4)	0.4 (0.0)	81.6 (4.8)
PMB30-adsorbed Co–Cr–Mo	70.6 (1.4)	24.1 (1.3)	2.3 (0.4)	3.0 (0.3)	0.0 (0.0)	0.0 (0.0)	0.0 (0.0)	0.0 (0.0)	95.8[b] (3.5)
PMSi90-immobilized Co–Cr–Mo	61.4 (0.9)	29.5 (0.7)	3.6 (0.4)	4.2 (0.1)	1.3 (0.4)	0.1 (0.2)	0.0 (0.0)	0.0 (0.0)	16.6[b] (2.4)
PMPC-grafted Co–Cr–Mo	61.7 (0.7)	28.0 (0.6)	5.0 (0.3)	5.3 (0.1)	0.1 (0.1)	0.0 (0.0)	0.0 (0.0)	0.0 (0.0)	23.5[b] (8.4)

[a] The standard deviations are shown in parentheses.
[b] Significant difference ($p < 0.001$) as compared to the untreated Co–Cr–Mo.

2.11. Statistical analysis

The results derived from each measurement in the water-contact angle measurement, friction test, and protein adsorption test were expressed as mean values ± standard deviation. The statistical significance ($p < 0.05$) was estimated by Student's *t*-test.

3. Results

Fig. 2 shows the FT-IR/ATR spectra of the surface-modified Co–Cr–Mo samples with various MPC polymers. Absorption peaks were newly observed for the surface-modified Co–Cr–Mo with MPC polymers. The peaks at 1720, 1550, and 1460 cm^{-1} are attributed to C = O and $-CH_2-$ in the MPC polymer. The peaks at 1180, 1040, 700, and 630 cm^{-1} are attributed to the trimethoxysilane group in the MPSi unit [19]. The peaks at 1240, 1080, 970, and 920 cm^{-1} are attributed to the $-N^+(CH_3)_3$ and phosphate groups in the MPC unit [22]. The absorption peak intensities of the phosphate groups of the PMPC-grafted Co–Cr–Mo were the highest in the Co–Cr–Mo whose surface was modified by the MPC polymer.

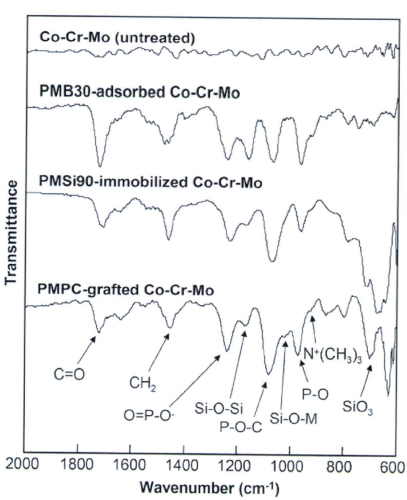

Fig. 2. FT-IR/ATR spectra of untreated Co–Cr–Mo, MPC polymer-coated Co–Cr–Mo, and PMPC grafted Co–Cr–Mo.

Table 1 summarizes the surface elemental composition and static-water contact angle of the surface-modified Co–Cr–Mo samples with various MPC polymers. The nitrogen (N) and phosphorous (P) contents in all the Co–Cr–Mo samples whose surfaces were modified by the MPC polymer were observed. The elemental compositions of both N and P in the surface-modified Co–Cr–Mo increased with an increase in the MPC composition in the polymer for surface modification. In particular, these values of N and P in the PMPC-grafted Co–Cr–Mo surface were 5.0 and 5.3 atom%, respectively, and were almost equivalent to the theoretical elemental composition (N = 5.3, P = 5.3 atom%) of PMPC. The static-water contact angle of the untreated Co–Cr–Mo was 81.6°, and this decreased markedly to approximately 20° (i.e., 16.6°–23.5°, $p < 0.001$) by the modifications with PMSi90 and PMPC.

Fig. 3 shows the cross-sectional TEM images of the surface-modified Co–Cr–Mo samples with various MPC polymers. For PMB30-adsorption, PMSi90-immobilization, and PMPC-grafting, a thickness of 50, 130, and 200 nm, respectively, of the MPC polymer layers was clearly observed on the surface of the Co–Cr–Mo substrate. No cracks due to poor adhesion and/or delamination were observed at the interface between the MPC polymer layer and Co–Cr–Mo substrate. These results indicate that each surface modification layer on the Co–Cr–Mo substrate is uniform and adheres closely, regardless of the binding conditions; the surface modification layers by PMB30-adsorption, PMSi90-immobilization, and PMPC-grafting combine with the substrate by physical adsorption and covalent bonds of Si–O–metal (M), respectively. However, in the PMB30-adsorbed Co–Cr–Mo, a bilayer structure for poor adhesion attributed to dipping twice was clearly observed on the surface modification layer. Further, in the PMB30-adsorbed and PMSi90-immobilized Co–Cr–Mo samples, a porous structure was clearly observed on the surface modification layer. This porous structure was also observed on the surface modification layer prepared by the slow-rate solvent evaporation method (approximately for 1 month at 4 °C, data not shown).

Fig. 4 shows the EDX spectra of the surface-modified Co–Cr–Mo samples with various MPC polymers. In spectra (b_{1-3}), (c_{1-3}), and (d_{1-3}) of the MPC polymer layers, a significant peak attributed to the P atom was observed at 2.0 keV. This peak is mainly attributed to the MPC units. Interestingly, this peak was clearly observed in spectra (b_2) and (c_2) of the porous part of the MPC polymer layer. In spectra (c_1) and (d_1) of the interface of the PMSi90-immobilization layer and the intermediate layer of the PMPC-grafted Co–Cr–Mo, peaks were observed at 0.5 and 1.7 keV. These peaks are attributed to the O and Si atoms in the interface/intermediate layer between the silane of the MPSi and the metal oxide of the Co–Cr–Mo.

Fig. 5 shows the amounts of BSA, γ-globulins, and fibrinogen adsorbed on the surface-modified Co–Cr–Mo samples with various

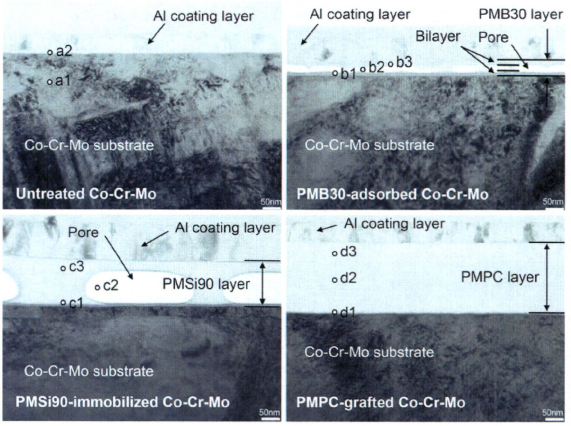

Fig. 3. Cross-sectional TEM images of the surface-modified Co–Cr–Mo with various MPC polymers. Aluminum coating layers (approximately 70–100 nm) for the preparation of TEM observation specimen are shown above the MPC polymer layer of the Co–Cr–Mo surface. Small open circles indicate EDX analysis points. Bar: 50 nm.

MPC polymers. The amount of each protein adsorbed on the Co–Cr–Mo surface modified by the MPC polymer was considerably lower ($p < 0.001$) than that on the untreated Co–Cr–Mo. These results imply that the surface modification by the MPC polymer results in good biocompatibility.

Fig. 6 shows the coefficients of dynamic friction of the sliding couples and articular cartilage pins sliding against the surface-modified Co–Cr–Mo plates with various MPC polymers. The PMB30-adsorbed and PMSi90-immobilized Co–Cr–Mo samples showed a slightly higher friction coefficient than the untreated Co–Cr–Mo sample in water at room temperature (not significantly different); in contrast, the MPC polymer-coated Co–Cr–Mo showed a lower friction coefficient than the untreated Co–Cr–Mo in BS mixture at 37 °C ($p < 0.05$). Further, the friction coefficient of the PMPC-grafted Co–Cr–Mo decreased drastically compared with untreated Co–Cr–Mo ($p < 0.001$) and reached approximately <0.010 in both lubricant conditions, i.e., water at room temperature and the BS mixture at 37 °C; moreover, it remained almost steady. The friction coefficients of all MPC polymer-containing BS mixtures were drastically lower as compared with that of non-additive BS mixture (Fig. 6).

Fig. 7 shows the coefficients of dynamic friction of the untreated Co–Cr–Mo and PMPC-grafted Co–Cr–Mo samples as a function of the loads. At both 10 and 100 cycles, the PMPC-grafted Co–Cr–Mo sample showed a remarkably low friction coefficient of approximately 0.019 at a load of 0.49 N; this value decreased gradually and reached approximately <0.010 at a load of 9.80 N. Similarly, the friction coefficients of the untreated Co–Cr–Mo sample in the initial 10 cycles decreased gradually from 0.188 to 0.045. However, this value of the untreated Co–Cr–Mo at 100 cycles decreased to 0.082 up to loads of 1.96 N; it then gradually increased with an increase in the loads. Fig. 7B shows the friction coefficients of the untreated Co–Cr–Mo and PMPC-grafted Co–Cr–Mo samples as a function of the test durations. It was observed that the friction coefficient was significantly lower in the PMPC-grafted Co–Cr–Mo sample than in the untreated Co–Cr–Mo one. This value was almost constant throughout the 5×10^3 cycles of the friction test.

Fig. 8 shows the histological findings of the articular cartilage pins after 5×10^3 cycles of friction tests. In the cartilage against the untreated Co–Cr–Mo, the cartilage layer of the worn surface became thicker as compared with the surrounding articular cartilage of the unworn surface. In contrast, in the cartilage against the PMPC-grafted Co–Cr–Mo, the layer of the worn surface did not differ considerably from that of the unworn surface.

Fig. 9 shows the time course of the surface modification layer of the untreated, MPC polymer-coated, and PMPC-grafted Co–Cr–Mo samples during PBS soaking. The elemental compositions of both N and P in the untreated, PMB30-adsorbed, and PMPC-grafted Co–Cr–Mo samples were almost constant throughout the 12 weeks of PBS soaking. In contrast, in the PMSi90-immobilized Co–Cr–Mo sample, these values decreased gradually with the PBS-soaking duration. Similarly, the static-water contact angle of untreated, PMB30-adsorbed, and PMPC-grafted Co–Cr–Mo samples were almost constant throughout PBS soaking, whereas the values in PMSi90-immobilized Co–Cr–Mo increased gradually.

Fig. 10 shows FM images of the surface-modified Co–Cr–Mo samples with various MPC polymers before and after friction tests/PBS-soaking tests. After 100 cycles of friction tests, the MPC polymer layer was removed from the PMB30-adsorbed and PMSi90-immobilized Co–Cr–Mo sliding surfaces; in contrast, most of the PMPC-grafted Co–Cr–Mo sliding surface was covered by the PMPC layer. After 12 weeks of PBS-soaking tests, most of the MPSi90 layer was removed from the Co–Cr–Mo surface, while most of the PMB30-adsorbed and PMPC-grafted Co–Cr–Mo surface was covered stably by the MPC polymer layer.

4. Discussion

In the hemi-arthroplasty, the highly lubricious surface by a "mild treatment" with soft materials was requested with aim of preserving the degradation of the articular cartilage. In this study, we have prepared various surface modification layers formed on the Co–Cr–Mo surface by MPC polymer coating or photoinduced radical polymerization of MPC to form PMPC graft chains for

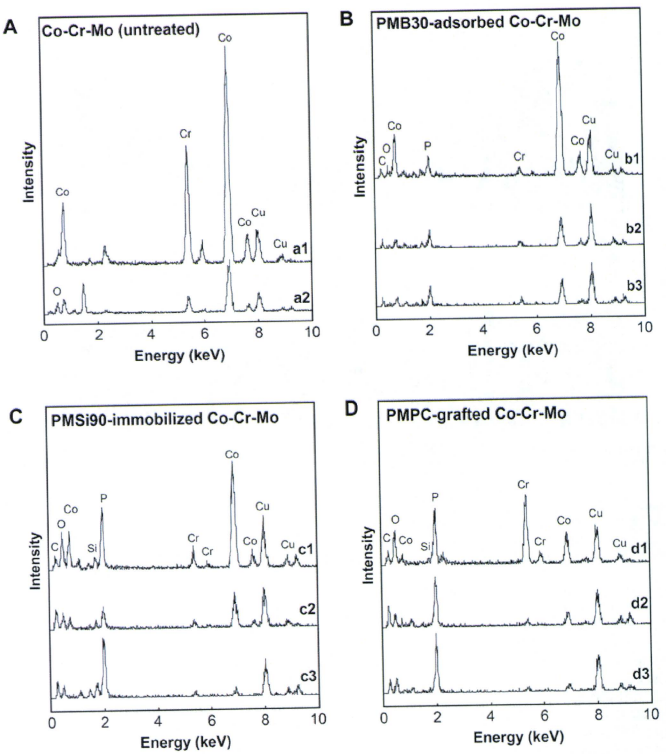

Fig. 4. EDX spectra of the untreated Co–Cr–Mo, MPC polymer-coated Co–Cr–Mo, and PMPC-grafted Co–Cr–Mo. The spectra were analyzed on the cross-section (small open circles in Fig. 3) of the untreated Co–Cr–Mo, MPC polymer-coated Co–Cr–Mo, and PMPC-grafted Co–Cr–Mo.

improving lubrication and preventing the degradation of acetabular cartilage. Here, we discuss the structures and stabilities of the surface modification layers of the MPC polymer and the effects of these characteristics on the retention of articular cartilage in hemiarthroplasty.

To ensure the *in vivo* long-term stability of the MPC modified layer on the Co–Cr–Mo surface, it is necessary to create strong covalent bonding between the Co–Cr–Mo substrate and the MPC polymer. Organosilanes have already been known as surface coupling agents that enhance bonding between a metal or a metal oxide surface and an organic resin such as dental resin; moreover, they can strongly bind metals to resins in dental implants [23]. Organic silanes or silane coupling agents comprise at least a hydrolyzable alkoxysilyl or chlorosilyl group and an organofunctional group. The agents are effective for introducing organofunctional groups into the siloxane network polymer. The organofunctional group in the silane could be useful for improving bonding with the organic overlayer. MPSi binds to the Co–Cr–Mo substrate by a condensation reaction in two steps; in the first step, MPSi is hydrolyzed (activated) and in the second step, the hydrolyzed silane molecule binds to the surface by an Si–O–M bond, forming branched hydrophobic siloxane bonds, i.e., Si–O–Si. The hydrolyzed silane molecule has three –OH groups that can react with the –OH groups of the surface metallic oxide layer to form siloxane bonds covalently. The peaks at 1180 and 1040 cm^{-1} in the FT-IR/ATR spectrum of the PMSi90-immobilized and PMPC-grafted Co–Cr–Mo surfaces were attributed to Si–O–Si and Si–O–M, respectively (Fig. 2).

However, several previous studies have reported that a silane coating has low water resistance due to hydrolysis of the siloxane bond and desorption of the physisorbed silane [24]. In fact, the PMSi90-immobilization layer was removed from the Co–Cr–Mo surface after 12 weeks of PBS soaking (Figs. 9 and 10). Zhang, et al. and others have reported that the water stability of Si–O–M could be improved by employing the following factors: (1) an induction of bridged silane coupling agents, when hydrolyzed, contain two or more $-Si(OH)_3$, (2) the hydrophobic alkyl moieties that limit the contact with water, and (3) an increase in the thickness of the

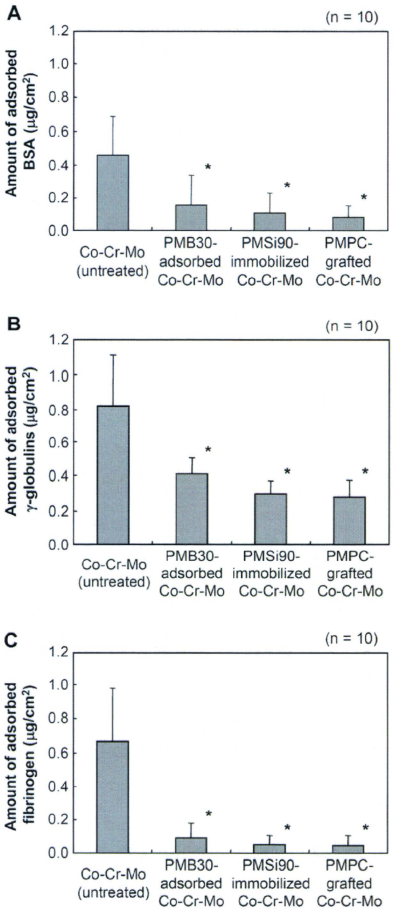

Fig. 5. Amounts of (A) BSA, (B) γ-globulins, and (C) fibrinogen adsorbed on the surfaces of the untreated Co–Cr–Mo, MPC polymer-coated Co–Cr–Mo, and PMPC-grafted Co–Cr–Mo. Bar: Standard deviations. *: Significant difference ($p < 0.001$) as compared to the untreated Co–Cr–Mo.

surface oxide layer [25]. Therefore, it was considered that the MPSi intermediate layer with a bridge of three methoxysilane groups with MPSi unit composition of 100% (MPSi unit of PMSi90 composition was 10% only) was essential in PMPC-grafted Co–Cr–Mo. Additionally, a functional methacrylate and pretreatment (nitric acid treatment and O_2 plasma treatment) for the Co–Cr–Mo surface were used. As shown in Figs. 9 and 10, the high stability of

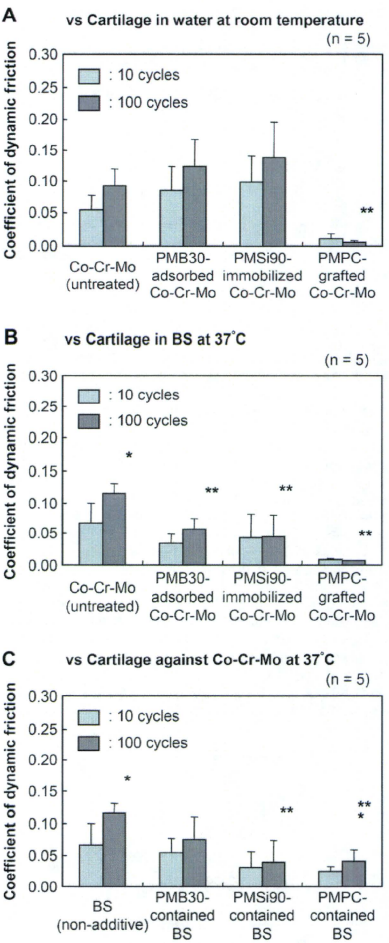

Fig. 6. Coefficients of dynamic friction of the untreated, MPC polymer-coated, and PMPC-grafted Co–Cr–Mo in the pin-on-plate friction test with various lubrication conditions. (A) Against cartilage pin with water at room temperature, (B) against cartilage pin with BS lubricant at 37 °C, (C) untreated Co–Cr–Mo plate against cartilage pin with BS lubricant with MPC polymer as additive at 37 °C. Bar: Standard deviations. *: *t*-test, significant difference ($p < 0.05$) as compared to the coefficients of dynamic friction at 10 cycles, and **: *t*-test, significant difference ($p < 0.05$) as compared to the untreated Co–Cr–Mo plate at 100 cycles.

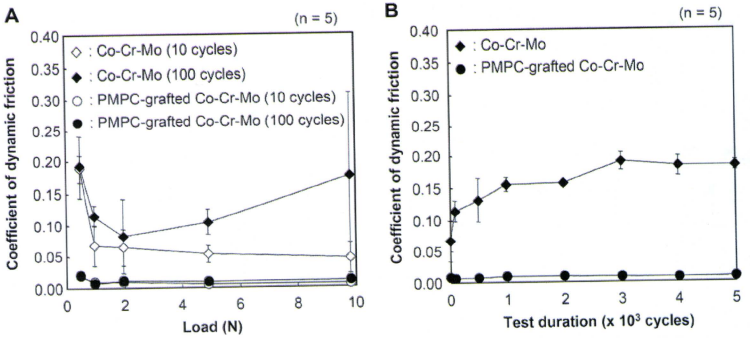

Fig. 7. Coefficients of dynamic friction of the untreated and PMPC-grafted Co–Cr–Mo in the pin-on-plate friction test. (A) Coefficients of dynamic friction of the untreated and PMPC-grafted Co–Cr–Mo against cartilage pin as a function of loads in the pin-on-plate friction test with BS lubricant at 37 °C. (B) Time course of coefficients of dynamic friction of the untreated and PMPC-grafted Co–Cr–Mo against the cartilage pin during 5×10^3 cycles of loading with 0.98 N in the pin-on-plate friction test with BS lubricant at 37 °C. Bar: Standard deviations.

the PMPC-grafted layer was confirmed throughout 12 weeks of PBS soaking.

On the other hand, the high stability of the PMB30-adsorbed layer was also confirmed throughout 12 weeks of PBS soaking. As shown in Table 1, the static-water contact angle of the PMB30-adsorbed Co–Cr–Mo was 95.8°. Sibarani et al. reported that the PMB30-adsorbed polymer surfaces showed high advancing (approximately 100°) and low receding (approximately 20°) contact angles: PMB30 cannot be hydrated easily due to the low MPC unit composition of the copolymer [10]. However, as shown in Fig. 5, the PMB30-adsorbed Co–Cr–Mo surface, which could form a phosphorylcholine-enriched surface after equilibrating for 1 h, showed excellent biocompatibility as an anti-protein adsorption surface. Hence, the PMB30-adsorbed layer has been observed to be stable (insoluble and attachable *in vivo* condition) and useful on several medical devices [14,15].

In Figs. 6 and 7, the PMPC-grafted Co–Cr–Mo surface shows an extremely low friction coefficient as compared to that of the untreated Co–Cr–Mo surface. Since MPC is highly hydrophilic and PMPC is water soluble, the water contact angle of the PMPC-grafted Co–Cr–Mo surface was lower than that of the untreated Co–Cr–Mo surface, as shown in Table 1. Consequently, the PMPC-grafted layer successfully provided high lubricity in the form of "surface gel hydration lubrication" to the Co–Cr–Mo surface (Fig. 3). A previous study has reported that the hydrogel cartilage surface is assumed to have a brush-like structure: a part of the proteoglycan brush is bonded with the collagen network on the cartilage surface [26]. The bearing surface with PMPC is assumed to have a brush-like structure similar to that of articular cartilage. Cartilage/PMPC-grafted Co–Cr–Mo bearing couples can therefore be regarded to be mimicking natural joint cartilage *in vivo*. The friction coefficient of cartilage/cartilage was reported to be approximately 0.01–0.02

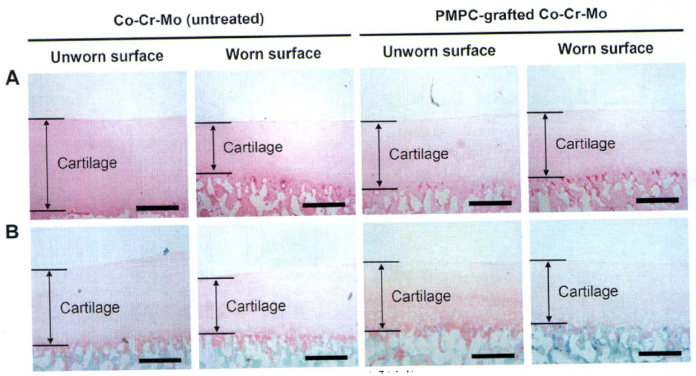

Fig. 8. Histological findings of the articular cartilage pins after 5×10^3 cycles of friction tests. (A) H&E stained, and (B) safranin-O stained. Bar; 500 μm.

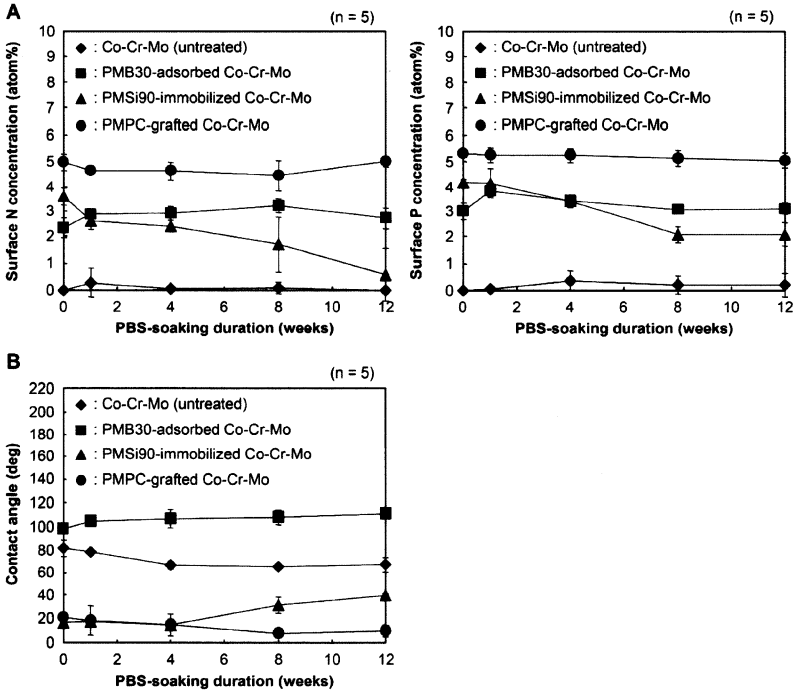

Fig. 9. Time course of the surface-modification layer of the untreated, MPC polymer-coated and PMPC-grafted Co–Cr–Mo during PBS soaking with 120 rpm shaking at 37 °C. (A) Surface N and P concentrations by XPS, and (B) static-water contact angle. Bar: Standard deviations.

[27,28]. In this study, it was found that the cartilage/PMPC-grafted Co–Cr–Mo interface mimicking a natural joint showed low friction (friction coefficient was <0.01), i.e., as low as that of cartilage/cartilage interface. Hence, it was considered that the PMPC-grafted Co–Cr–Mo surface is well suited for application on the artificial femoral head that would chafe against articulating cartilage. We expect that hemi-arthroplasty with a PMPC-grafted Co–Cr–Mo femoral head will be a promising option that preserves acetabular cartilage and extends the duration before total hip arthroplasty (THA) in young patients. Moreover, we consider that these effects would occur continuously. In Fig. 7B, the friction coefficient shows a test duration-dependent response for articular cartilage against the untreated Co–Cr–Mo sample due to the continued loading of the cartilage tissue and the ensuing loss of fluid-film formation (or rehydration). It was thought that the thickness of the cartilage tissue atrophied due to the fairly poor access of the cartilage tissue to water (Fig. 8). Decreased water content often leads to the degradation of cartilage function. Although cartilage tissues are able to produce matrix components throughout life, i.e., carry out regeneration, their production cannot keep pace with the repair requirements after acute damage to articular cartilage; such damages limit the longevity of the artificial femoral head and its stability after hemi-arthroplasty. In contrast, in articular cartilage against the PMPC-grafted Co–Cr–Mo sample, the friction coefficient remained at a steady low value due to the rehydration of the continuously loaded cartilage tissue, and the articular cartilage surface was preserved.

In Fig. 6A, the PMB30-adsorbed and PMSi90-immobilized Co–Cr–Mo samples show a slightly higher friction coefficient than the untreated Co–Cr–Mo sample in water at room temperature. Some pores in the PMB30 and PMSi90 layers on the Co–Cr–Mo surface could be observed (Fig. 3); these may have occurred due to the low density of the material because physical adsorption or chemical immobilization of the polymer was used as the surface modification method. Therefore, it is assumed that a sliding couple with cartilage and low-density MPC polymer layer may cause high friction by stick-slip motion with interpenetration [18]. Furthermore, the MPC polymer-coated Co–Cr–Mo showed a lower friction coefficient than the untreated Co–Cr–Mo in BS mixture at 37 °C (Fig. 6B). It was thought that the interpenetration of cartilage and low-density MPC polymer layer was blocked by the protein of BS presented between the interfaces. In contrast, the friction coefficient of the PMPC-grafted Co–Cr–Mo sample was drastically as compared with that of the untreated Co–Cr–Mo sample; the degree

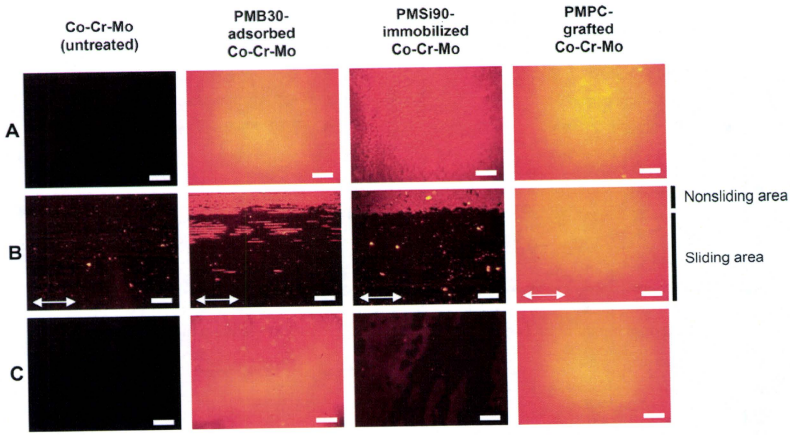

Fig. 10. FM images of the untreated Co–Cr–Mo, MPC polymer-coated Co–Cr–Mo, and PMPC-grafted Co–Cr–Mo surfaces. FM images of the surface before tests (A), after 100 cycles of friction tests with BS lubricant (B), and after 12 weeks of PBS-soaking tests (C). Bar; 200 μm. Arrow; Sliding direction of friction test.

of reduction in the coefficient was 93%. PMPC-grafted Co–Cr–Mo might have a high density because the polymerization method used was surface-initiated graft polymerization, termed as the "grafting from" method [19,29]. A sliding couple with cartilage tissue and high-density PMPC layer fabricated by the "grafting from" method may be responsible for low friction, such as that in the case of "super-lubricity," because of resistance to interpenetration by volume effects resulting from the mobility of hydrophilic macromolecules of cartilage tissue and the PMPC-grafted layer [30–32].

As shown in Fig. 7A, the friction coefficients of the articular cartilage against the untreated and PMPC-grafted Co–Cr–Mo samples decreased with an increasing load in the initial 10 cycles. The elastic articular cartilage tissue and PMPC-grafted layer was slightly deformed by the loads; the low friction coefficient might occur in order to increase the contact area of the fluid film's concave surface. However, the friction coefficient of the articular cartilage against the untreated Co–Cr–Mo at 100 cycles decreased to 0.082 up to loads of 1.96 N; a further increase in loads up to 9.8 N resulted in elevated friction coefficients. Under a high load, water exudes slowly from the articular cartilage with sliding [27]. As the result of water loss, the thickness of the surface layer and/or fluid film reduces, and the water content of the surface-hydration layer decreases. Consequently, the degree of adhesion of articular cartilage to the Co–Cr–Mo surface increases due to a lack of rehydration and because of the increase in frictional force. In contrast, the PMPC-grafted Co–Cr–Mo sample at 100 cycles showed a remarkably low friction coefficient that reached approximately <0.010 at a load of 9.80 N. We consider that this result implies that the rehydration and hydrodynamic lubrication mechanism of the articular cartilage is supported by the hydrated PMPC-grafted layer, similar to the interface between cartilage/cartilage of the natural joint.

The friction coefficients of cartilage/untreated Co–Cr–Mo interface with all MPC polymer-containing BS mixtures as a lubricant were drastically lower as compared with that with the non-additive BS mixture (Fig. 6C). Synovial fluid as a whole, and all its components such as hyaluronic acid, glycoprotein (mainly lubricin), and surface-active phospholipids, have been proposed as lubricants responsible for boundary lubrication in the natural joint [33]. Similarly, it is considered that the additives of MPC polymer would play the role akin to synovial phospholipids for boundary lubrication, and the adsorption of the MPC polymer to the sliding surface could prevent direct contact between the cartilage and the untreated Co–Cr–Mo and hence decrease the frictional force between them. However, in the case of additives, the lubricity may change depending on the ambient *in vitro* and *in vivo* conditions, because the additives probably diffuse to synovial fluid *in vivo*.

The amounts of the representative protein, BSA, γ-globulins, and fibrinogen, adsorbed on the modified Co–Cr–Mo surface with the MPC polymer were significantly low, these reached to 7%–50% of that of the untreated surface, as shown in Fig. 5. It is hypothesized that the mechanism underlying protein adsorption resistivity of a surface modified by the MPC polymer is based on the water structure resulting from the interactions between water molecules and phosphorylcholine groups [34]. The large amount of free water around the phosphorylcholine group is considered to detach proteins easily and prevent conformational changes in the adsorbed proteins even when the proteins attached to the surface [3,34]. The reduction in protein adsorption is also considered to be caused by the presence of a hydrated layer around the phosphorylcholine group [35]. The latter consideration is consistent with the results of the water contact angle measurement, friction test, and TEM and FM observations of the Co–Cr–Mo samples whose surfaces were modified by the MPC polymer. It should be noted that the porous structure (low density) of the PMB30-adsorption and PMSi90-immobilization layer (in dry conditions) hardly affected the protein adsorption. Therefore, the Co–Cr–Mo sample whose surface is modified by the MPC polymer is expected to exhibit tissue and blood compatibility, i.e., biocompatibility, because previous studies have reported that the MPC polymer-modified surfaces exhibit *in vivo* biocompatibility [6–16].

5. Conclusions

In this study, we systematically investigated the surface properties of the various surface modification layers formed on the Co–Cr–Mo surface by the MPC polymer by dip coating or photoinduced radical grafting. We conclude that several important issues are involved in the long-term retention of the benefits of the MPC polymer used in artificial joints under variable and multidirectional loads, for example, strong bonding between the MPC polymer and the Co–Cr–Mo surface as also a high density of the MPC polymer. We suggest that the MPSi intermediate layer and photoinduced radical graft polymerization should be employed to create strong covalent bonding between the surface modification layer and Co–Cr–Mo substrate and to retain the high density of the polymer chains of that layer. The cartilage/PMPC-grafted Co–Cr–Mo interface, which mimicked a natural joint, showed an extremely low friction coefficient of <0.01, a value as low as that of a natural cartilage interface. We expect that the PMPC-grafted Co–Cr–Mo femoral head for hemi-arthroplasty will be a promising option for preserving acetabular cartilage and extending the duration before THA.

Acknowledgements

This study was supported by the Health and Welfare Research Grant for Translational Research (H17-005), Research on Medical Devices for Improving Impaired QOL (H20-004) from the Japanese Ministry of Health, Labour and Welfare. We thank Mr. Y. Yoshihara and Ms. Y. Nakao, Japan Medical Materials Corporation, for their excellent technical assistance.

Appendix

Figures with essential colour discrimination. Certain figures in this article, in particular Figures 8 and 10, are difficult to interpret in black and white. The full colour images can be found in the on-line version, at doi:10.1016/j.biomaterials.2009.09.083.

References

[1] Healy WL, Lemos DW, Appleby D, Lucchesi CA, Saleh KJ. Displaced femoral neck fractures in the elderly: outcomes and cost effectiveness. Clin Orthop Relat Res 2001;383:229–42.
[2] Beaulé PE, Amstutz HC, Le Duff M, Dorey F. Surface arthroplasty for osteonecrosis of the hip: hemiresurfacing versus metal-on-metal hybrid resurfacing. J Arthroplasty 2004;19(8 Suppl. 3):54–8.
[3] Kyomoto M, Moro T, Miyaji F, Hashimoto M, Kawaguchi H, Takatori Y, et al. Effects of mobility/immobility of surface modification by 2-methacryloyloxyethyl phosphorylcholine polymer on the durability of polyethylene for artificial joints. J Biomed Mater Res A 2009;90(2):362–71.
[4] Kyomoto M, Moro T, Miyaji F, Hashimoto M, Kawaguchi H, Takatori Y, et al. Effect of 2-methacryloyloxyethyl phosphorylcholine concentration on photoinduced graft polymerization of polyethylene in reducing the wear of orthopaedic bearing surface. J Biomed Mater Res A 2008;86(2):439–47.
[5] Kyomoto M, Moro T, Miyaji F, Konno T, Hashimoto M, Kawaguchi H, et al. Enhanced wear resistance of orthopedic bearing due to the cross-linking of poly(MPC) graft chains induced by gamma-ray irradiation. J Biomed Mater Res B Appl Biomater 2008;84(2):320–7.
[6] Moro T, Takatori Y, Ishihara K, Konno T, Takigawa Y, Matsushita T, et al. Surface grafting of artificial joints with a biocompatible polymer for preventing periprosthetic osteolysis. Nature Mater 2004;3:829–37.
[7] Moro T, Takatori Y, Ishihara K, Nakamura K, Kawaguchi H. 2006 Frank Stinchfield Award: grafting of biocompatible polymer for longevity of artificial hip joints. Clin Orthop Relat Res 2006;453:58–63.
[8] Moro T, Kawaguchi H, Ishihara K, Kyomoto M, Karita T, Ito H, et al. Wear resistance of artificial hip joints with poly(2-methacryloyloxyethyl phosphorylcholine) grafted polyethylene: comparisons with the effect of polyethylene cross-linking and ceramic femoral heads. Biomaterials 2009;30(16):2995–3001.
[9] Kyomoto M, Ishihara K. Self-initiated surface graft polymerization of 2-methacryloyloxyethyl phosphorylcholine on poly(ether–ether–ketone) by photo-irradiation. ACS Appl Mater Interfaces 2009;1(3):537–42.
[10] Sibarani J, Takai M, Ishihara K. Surface modification on microfluidic devices with 2-methacryloyloxyethyl phosphorylcholine polymers for reducing unfavorable protein adsorption. Colloids Surf B Biointerfaces 2007;54(1):88–93.
[11] Ueda T, Oshida H, Kurita K, Ishihara K, Nakabayashi N. Preparation of 2-methacryloyloxyethyl phosphorylcholine copolymers with alkyl methacrylates and their blood compatibility. Polym J 1992;24(11):1259–69.
[12] Konno T, Ishihara K. Temporal and spatially controllable cell encapsulation using a water-soluble phospholipid polymer with phenylboronic acid moiety. Biomaterials 2007;28(10):1770–7.
[13] Xu Y, Takai M, Konno T, Ishihara K. Microfluidic flow control on charged phospholipid polymer interface. Lab Chip 2007;7(2):199–206.
[14] Snyder TA, Tsukui H, Kihara S, Akimoto T, Litwak KN, Kameneva MV, et al. Preclinical biocompatibility assessment of the EVAHEART ventricular assist device: coating comparison and platelet activation. J Biomed Mater Res A 2007;81(1):85–92.
[15] Ueda H, Watanabe J, Konno T, Takai M, Saito A, Ishihara K. Asymmetrically functional surface properties on biocompatible phospholipid polymer membrane for bioartificial kidney. J Biomed Mater Res A 2006;77(1):19–27.
[16] Kyomoto M, Moro T, Konno T, Takadama H, Yamawaki N, Kawaguchi H, et al. Enhanced wear resistance of modified cross-linked polyethylene by grafting with poly(2-methacryloyloxyethyl phosphorylcholine). J Biomed Mater Res A 2007;82(1):10–7.
[17] Ishihara K, Ueda T, Nakabayashi N. Preparation of phospholipid polymers and their properties as polymer hydrogel membranes. Polym J 1990;22(5):355–60.
[18] Kyomoto M, Iwasaki Y, Moro T, Konno T, Miyaji F, Kawaguchi H, et al. High lubricious surface of cobalt–chromium–molybdenum alloy prepared by grafting poly(2-methacryloyloxyethyl phosphorylcholine). Biomaterials 2007;28(20):3121–30.
[19] Kyomoto, M., Moro, T., Iwasaki, Y., Miyaji, F., Kawaguchi, H., Takatori, Y., et al. Superlubricious surface mimicking articular cartilage by grafting poly(2-methacryloyloxyethyl phosphorylcholine) on orthopaedic metal bearings. J Biomed Mater Res A, in press.
[20] Wang JH, Bartlett JD, Dunn AC, Small S, Willis SL, Driver MJ, et al. The use of rhodamine 6G and fluorescence microscopy in the evaluation of phospholipid-based polymeric biomaterials. J Microsc 2005;217(Pt 3):216–24.
[21] Arendt SA, Bailey SJ, editors. ASTM F732–00: standard test method for wear testing of polymeric materials used in total joint prostheses. Annual book of ASTM standards, vol. 13; 2004.
[22] Kyomoto M, Moro T, Konno T, Takadama H, Kawaguchi H, Takatori Y, et al. Effects of photo-induced graft polymerization of 2-methacryloyloxyethyl phosphorylcholine on physical properties of cross-linked polyethylene in artificial hip joints. J Mater Sci Mater Med 2007;18:1809–15.
[23] Yoshida K, Greener EH. Effects of coupling agents on mechanical properties of metal oxide-polymethacrylate composites. J Dent 1994;22:57–62.
[24] Matinlinna JP, Vallittu PK. Bonding of resin composites to etchable ceramic surfaces – an insight review of the chemical aspects on surface conditioning. J Oral Rehabil 2007;34(8):622–30.
[25] Zhang Z, Berns AE, Willbold S, Buitenhuis J. Synthesis of poly(ethylene glycol) (PEG)-grafted colloidal silica particles with improved stability in aqueous solvents. J Colloid Interface Sci 2007;310(2):446–55.
[26] Ishikawa Y, Hiratsuka K, Sasada T. Role of water in the lubrication of hydrogel. Wear 2006;261:500–4.
[27] Katta J, Jin Z, Ingham E, Fisher J. Biotribology of articular cartilage – a review of the recent advances. Med Eng Phys 2008;30(10):1349–63.
[28] Bell CJ, Ingham E, Fisher J. Influence of hyaluronic acid on the time-dependent friction response of articular cartilage under different conditions. Proc Inst Mech Eng [H] 2006;220(1):23–31.
[29] Matsuda T, Kaneko M, Ge S. Quasi-living surface graft polymerization with phosphorylcholine group(s) at the terminal end. Biomaterials 2003;24:4507–15.
[30] Raviv U, Glasson S, Kampf N, Gohy JF, Jérôme R, Klein J. Lubrication by charged polymers. Nature 2003;425:163–5.
[31] Chen M, Briscoe WH, Armes SP, Klein J. Lubrication at physiological pressures by polyzwitterionic brushes. Science 2009;323(5922):1698–701.
[32] Kobayashi M, Terayama Y, Hosaka N, Kaido M, Suzuki A, Yamada N, et al. Friction behavior of high-density poly(2-methacryloyloxyethyl phosphorylcholine) brush in aqueous media. Soft Matter 2007;2:740–6.
[33] Sawae Y, Yamamoto A, Murakami T. Influence of protein and lipid concentration of the test lubricant on the wear of ultra high molecular weight polyethylene. Tribol Int 2008;41(7):648–56.
[34] Goda T, Konno T, Takai M, Ishihara K. Photoinduced phospholipid polymer grafting on Parylene film: advanced lubrication and antibiofouling properties. Colloids Surf B Biointerfaces 2007;54(1):67–73.
[35] Hoshi T, Sawaguchi T, Konno T, Takai M, Ishihara K. Preparation of molecular dispersed polymer blend composed of polyethylene and poly(vinyl acetate) by in situ polymerization of vinyl acetate using supercritical carbon dioxide. Polymer 2007;48(6):1573–80.

Biomaterials 31 (2010) 1017–1024

Contents lists available at ScienceDirect

Biomaterials

journal homepage: www.elsevier.com/locate/biomaterials

Self-initiated surface grafting with poly(2-methacryloyloxyethyl phosphorylcholine) on poly(ether-ether-ketone)

Masayuki Kyomoto [a,b,e], Toru Moro [b,c], Yoshio Takatori [b,c], Hiroshi Kawaguchi [c], Kozo Nakamura [c], Kazuhiko Ishihara [a,d,*]

[a] Department of Materials Engineering, School of Engineering, The University of Tokyo, 7-3-1, Hongo, Bunkyo-ku, Tokyo 113-8656, Japan
[b] Division of Science for Joint Reconstruction, Graduate School of Medicine, The University of Tokyo, 7-3-1, Hongo, Bunkyo-ku, Tokyo 113-8655, Japan
[c] Sensory & Motor System Medicine, Faculty of Medicine, The University of Tokyo, 7-3-1, Hongo, Bunkyo-ku, Tokyo 113-8655, Japan
[d] Center for NanoBio Integration, The University of Tokyo, 7-3-1, Hongo, Bunkyo-ku, Tokyo 113-8656, Japan
[e] Research Department, Japan Medical Materials Corporation, 3-3-31, Miyahara, Yodogawa-ku, Osaka 532-0003, Japan

ARTICLE INFO

Article history:
Received 20 August 2009
Accepted 25 October 2009
Available online 10 November 2009

Keywords:
Polyetheretherketone
Phosphorylcholine
Surface modification
Photopolymerization
Protein adsorption
Friction

ABSTRACT

Poly(ether-ether-ketone) (PEEK)s are a group of polymeric biomaterials with excellent mechanical properties and chemical stability. In the present study, we demonstrate the fabrication of an antibiofouling and highly hydrophilic high-density nanometer-scaled layer on the surface of PEEK by photo-induced graft polymerization of 2-methacryloyloxyethyl phosphorylcholine (MPC) without using any photo-initiators, i.e., "self-initiated surface graft polymerization." Our results indicated that the diphenylketone moiety in the polymer backbone acted as a photo-initiator similar to benzophenone. The density and thickness of the poly(MPC) (PMPC)-grafted layer were controlled by the photo-irradiation time and monomer concentration during polymerization, respectively. Since MPC is a highly hydrophilic compound, the water wettability (contact angle $<10°$) and lubricity (coefficient of dynamic friction <0.01) of the PMPC-grafted PEEK surface were considerably lower than those of the untreated PEEK surface (90° and 0.20, respectively) due to the formation of a PMPC nanometer-scale layer. In addition, the amount (0.05 $\mu g/cm^2$) of BSA adsorbed on the PMPC-grafted PEEK surface was considerably lower, that is more than 90% reduction, compared to that (0.55 $\mu g/cm^2$) for untreated PEEK. This photo-induced polymerization process occurs only on the surface of the PEEK substrate; therefore, the desirable mechanical properties of PEEK would be maintained irrespective of the treatment used.

© 2009 Elsevier Ltd. All rights reserved.

1. Introduction

Poly(aryl-ether-ketone) (PAEK), including poly(ether-ether-ketone) (PEEK), is a new family of high performance thermoplastic polymers, consisting of an aromatic backbone molecular chain interconnected by ketone and ether functional groups, i.e., a benzophenone (BP) unit is included in its molecular structure. Polyaromatic ketones exhibit enhanced mechanical properties, and their chemical structure is stable, resistant to chemical and radiation damage, and compatible with several reinforcing agents (such as glass and carbon fibers); therefore, they are considered to be promising materials for not only industrial applications but also biomedical applications. In the 1980s, the *in vivo* stability of various PAEK materials and the tissue response to those were investigated [1]. Recently, PEEK has emerged as the leading high-performance super-engineering plastic candidate for replacing metal implant components, especially in the field of orthopedics and spinal surgery [2]. In recent studies, the tribological and bioactive properties of PEEK, which is used as a bearing material and flexible implant in orthopedic and spinal surgeries, has been investigated [3–5]. However, conventional single-component PEEK cannot satisfy these requirements (e.g., antibiofouling, wear resistance, and fixation to a bone) for use as an artificial joint or intervertebral body fusion cage [2]. For further improving the capabilities of PEEK as an implant biomaterial, various studies have focused upon the lubricity and antibiofouling of the polymer, either via reinforcing agents or surface modifications [6,7]. Therefore, multicomponent polymer systems have been designed in order to synthesize new multifunctional biomaterials. In order to use PEEK and related composites in the implant applications, they can be engineered to have a wide range of physical, mechanical, and surface properties.

* Corresponding author. Department of Materials Engineering, School of Engineering, The University of Tokyo, Hongo 7-3-1, Bunkyo-ku, Tokyo 113-8656, Japan. Tel.: +81 3 5841 7124; fax: +81 3 5841 8647.
E-mail address: ishihara@mpc.t.u-tokyo.ac.jp (K. Ishihara).

0142-9612/$ – see front matter © 2009 Elsevier Ltd. All rights reserved.
doi:10.1016/j.biomaterials.2009.10.055

Surface modification is one of the most important technologies for the preparation of new multifunctional biomaterials for satisfying several requirements; surface modifications used today include coating, blending, and grafting. In general, graft polymerization is performed most frequently using either of the following methods that utilize chemical and/or physical processes: (a) surface-initiated graft polymerization or "grafting from" methods in which the monomers are polymerized from initiators or comonomers, and (b) adsorption of the polymer to the substrate or "grafting to" methods, such as reaction of the end groups of the ready-made polymers with the functional groups of the substrate. The "grafting from" method has an advantage over the "grafting to" method wherein it forms a high-density polymer brush interface with a multifunctional polymer; this advantage proves to be functionally effective.

It is well known that when BP is exposed to photo-irradiation such as ultraviolet-ray (UV)-irradiation, a pinacolization reaction is induced; this results in the formation of semi-benzopinacol radicals (i.e., ketyl radicals) that act as photo-initiators. Therefore, in this study, we have focused upon a BP unit in PEEK and formulated a self-initiated surface-graft polymerization method that utilizes the BP unit in graft-from polymerization (Fig. 1) [8]. This polymerization reaction involving free radicals is photo-induced by UV-irradiation. Under UV-irradiation, a BP unit in PEEK can undergo the following reactions in the monomer aqueous solutions [9–15]: the pinacolization reaction (photo-reduction by the H-abstraction of a BP unit in PEEK) results in the formation of a semi-benzopinacol radical, which can initiate the graft-from polymerization of the feed monomer as the main reaction, and the graft-to polymerization (the radical chain end of the active-polymer couples with the semi-benzopinacol radical of the PEEK surface) as a sub-reaction. In addition, a photo-scission reaction occurs as a sub-reaction, which may not need an hydrogen (H)-donor. The cleavage reaction induces recombination and the graft-from polymerization. When water polymerization is performed in the presence of an H-donor, a phenol unit may be sub-sequentially formed due to H-abstraction. This technique enables the direct grafting of the functional polymer onto the PEEK surface in the absence of a photo-initiator, thereby resulting in the formation of a C–C covalent bond between the functional polymer and PEEK substrate.

2-Methacryloyloxyethyl phosphorylcholine (MPC), a methacrylate monomer bearing a phosphorylcholine group, is used to synthesize polymer biomaterials having excellent biocompatibility [16–25]; the MPC polymers have potential applications in a variety of fields such as biomedical science, surface science, and bioengineering because they possess unique properties such as excellent antibiofouling, and low friction abilities. Thus, surface modification with the MPC polymer on medical devices is effective for obtaining biocompatibility. Several medical devices have already been developed by utilizing MPC polymers and have been used clinically; therefore, the efficacy and safety of MPC polymers as biomaterials are well-established [23–25].

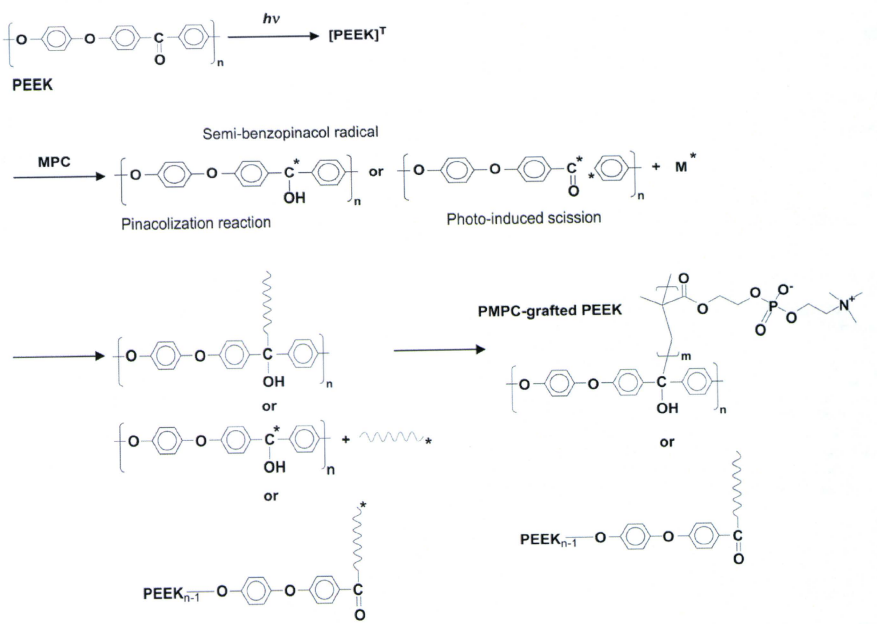

Fig. 1. Schematic illustration for the preparation of PMPC-grafted PEEK.

In this study, we have demonstrated the fabrication of a biocompatible and highly hydrophilic nanometer-scale-modified surface by poly(MPC) (PMPC)-grafting onto the self-initiated PEEK surface using a photo-induced pinacolization reaction; further, we also investigated the effects of photo-irradiation time and MPC concentration variability on PMPC-graft polymerization. The results revealed that it was possible to control the PMPC-graft layer in order to improve wettability, lubricity, and anti-protein adsorption for developing multifunctional PEEK biomaterials.

2. Materials and methods

2.1. Self-initiated graft polymerization of MPC

The preparation of PMPC-grafted PEEK is schematically illustrated in Fig. 1. PEEK specimens were machined from an extruded PEEK (450 G; Victrex PLC, Thornton-Cleveleys, UK) bar stock, which was fabricated without stabilizers or additives. The surfaces of the PEEK specimens were ultrasonically cleaned in ethanol for 20 min, and then dried in vacuum. MPC was industrially synthesized using the method reported by Ishihara et al. [26] and supplied by NOF Corp. (Tokyo, Japan). It was dissolved in degassed water to obtain 0.25- and 0.50-mol/L MPC aqueous solutions, and PEEK specimens were immersed in these solutions. Photo-induced graft polymerization was carried out at 60 °C for 5–90 min on the PEEK surface under UV-irradiation (UVL-400HA ultra-high pressure mercury lamp; Riko-Kagaku Sangyo Co. Ltd., Funabashi, Japan) with an intensity of 5 mW/cm^2; a filter (model D-35; Toshiba Corp., Tokyo, Japan) was used to restrict the passage of UV-light to wavelengths of 350 ± 50 nm. After polymerization, the PMPC-grafted PEEK specimens were removed from the reaction solution, washed with pure water and ethanol to remove non-reacted monomers and non-grafted polymers, and dried at room temperature.

2.2. Surface analysis of PMPC-grafted PEEK

The functional group vibrations of the PMPC-grafted PEEK surfaces were examined by Fourier-transform infrared (FT-IR) spectroscopy with attenuated total reflection (ATR) equipment. The FT-IR/ATR spectra were obtained using an FT-IR analyzer (FT/IR615; JASCO Co. Ltd., Tokyo, Japan) for 32 scans over the range of 1000–1800 cm^{-1} at a resolution of 4.0 cm^{-1}.

The surface elemental conditions of the PMPC-grafted PEEK surfaces were analyzed by X-ray photoelectron spectroscopy (XPS). The XPS spectra were obtained using an XPS spectrophotometer (AXIS-HSi165; Kratos/Shimadzu Co., Kyoto, Japan) equipped with a 15-kV Mg-K_α radiation source at the anode. The take-off angle of the photoelectrons was maintained at 90°. Five scans were taken for each sample.

The static-water contact angles on the PMPC-grafted PEEK surfaces were measured by the sessile drop method using an optical bench-type contact angle goniometer (Model DM300; Kyowa Interface Science Co. Ltd., Saitama, Japan). Drops of purified water (1.0 μL) were deposited on the PMPC-grafted PEEK surfaces, and the contact angles were directly measured with a microscope after 60 s of dropping. Measurements were repeated fifteen times for each sample, and the average values were regarded as the contact angles.

2.3. Cross-sectional observation by transmission electron microscopy

A cross-section of the PMPC layer on the PMPC-grafted PEEK surface was observed using a transmission electron microscope (TEM). The specimens were first embedded in epoxy resin, stained with ruthenium oxide vapor at room temperature, and then sliced into ultra-thin films (approximately 100-nm thick) by using a Leica Ultra Cut UC microtome (Leica Microsystems, Ltd., Wetzlar, Germany). A JEM-1010 electron microscope (JEOL, Ltd., Tokyo, Japan) was used for the TEM observation at an acceleration voltage of 100 kV. The thickness of the PMPC layer was determined by averaging ten points on the cross-sectional TEM image.

2.4. Gravimetric measurement of PMPC-grafted layer

The PMPC-grafted PEEK specimens were weighed on a microbalance (Sartorius Supermicro S4; Sartorius AG, Goettingen, Germany) to determine the physical properties of the PMPC-grafted layer. The physical properties were obtained by the following equations:

$$\text{PMPC} - \text{graftextent}(\text{g/cm}^2) = (W_g - W_0)/S \quad (1)$$

$$\text{PMPC} - \text{graftlayerdensity}(\text{g/cm}^3) = (W_g - W_0)/S \times T \quad (2)$$

where W_0 is the initial weight of the untreated PEEK substrate, W_g is the weight of the PMPC-grafted PEEK in dry condition, S is the grafted surface area of the PEEK substrate, and T is the thickness of the PMPC-graft layer determined by cross-sectional TEM observation. The weighing was repeated five times for each sample, and the average values were regarded as the weight of the samples.

2.5. Characterization of protein adsorption by micro-bicinchoninic acid method

The amount of protein adsorbed on the PMPC-grafted PEEK surfaces was measured by the micro-bicinchoninic acid (BCA) method. Each specimen was immersed in Dulbecco's phosphate-buffered saline (PBS, pH 7.4, ion strength = 0.15 M; Immuno-Biological Laboratories Co. Ltd., Takasaki, Japan) for 1 h to equilibrate the PMPC-grafted surface. The specimens were immersed in bovine serum albumin (BSA, $M_w = 6.7 \times 10^4$; Sigma-Aldrich Corp., MO, USA) solution at 37 °C for 1 h. The protein solution was prepared in a BSA concentration of 4.5 g/L, i.e., 10% of the concentration of human plasma levels. Then, the specimens were rinsed five times with fresh PBS and immersed in 10.0 g/L sodium dodecyl sulfate (SDS) aqueous solution and shaken at room temperature for 1 h to completely detach the adsorbed BSA on the PMPC-grafted surface. A protein analysis kit (micro BCA protein assay kit, #23235; Thermo Fisher Scientific Inc., IL, USA) based on the BCA method was used to determine the BSA concentration in the SDS solution, and the amount of BSA adsorbed on the PMPC-grafted PEEK surface was calculated.

2.6. Friction test

The friction test was performed using a pin-on-plate machine (Tribostation 32; Shinto Scientific Co. Ltd., Tokyo, Japan). Each of the PMPC-grafted PEEK surfaces was used to prepare five sample pieces. A 9-mm-diameter pin with Co-Cr-Mo alloy was prepared. The surface roughness (R_a) of the pin was <0.01, which was comparable to that of femoral head products. The friction tests were performed at room temperature with a load of 0.98 N, sliding distance of 25 mm, and a frequency of 1 Hz for a maximum of 100 cycles. Pure water was used as a lubricant. The mean coefficients of dynamic friction were determined by averaging five data points from the 100 (96–100) cycle measurements.

2.7. Mechanical test

The mechanical properties of untreated PEEK and PMPC-grafted PEEK with a 0.50-mol/L MPC concentration and 90-min photo-irradiation time were evaluated with tensile and flexural tests. Tensile testing was performed according to ISO527 standard using a type 1B tensile bar specimen and a crosshead speed of 50 mm/min. Flexural testing was performed according to ISO178 standard with a crosshead speed of 2 mm/min. The results derived from each measurement in the mechanical test were expressed as the mean values ± standard deviation. The statistical significance ($p < 0.05$) was estimated by Student's t-test.

3. Results

Fig. 2 shows the FT-IR/ATR and XPS spectra of untreated PEEK and PMPC-grafted PEEK with a 0.50-mol/L MPC concentration and 90-min photo-irradiation time. Transmission absorption peaks were observed at 1600, 1490, 1280, 1190, and 1160 cm^{-1} for both untreated PEEK and PMPC-grafted PEEK (Fig. 2(A)). These peaks are chiefly attributed to the diphenyl ether group, phenyl rings, or aromatic hydrogens in the PEEK substrate [8,27]. However, absorption peaks at 1720 and 1080 cm^{-1} (shoulder peak) were observed only for PMPC-grafted PEEK. These peaks corresponded to the carbonyl group (C=O) and phosphate group (P–O) in the MPC unit, respectively [8,25]. The XPS spectra of the binding energy region of the nitrogen (N) and phosphorous (P) electrons showed peaks for untreated PEEK and PMPC-grafted PEEK, whereas, peaks were not observed in the case of untreated PEEK (Fig. 2(B)). The peaks at 403 and 134 eV were attributed to the $-N^+(CH_3)_3$ and phosphate groups, respectively. These peaks indicate the presence of phosphorylcholine in the MPC units. After PMPC-grafting, the peaks attributed to the MPC unit were clearly observed in both the FT-IR/ATR and XPS spectra of the PMPC-grafted PEEK. These results indicate that PMPC was successfully grafted on the PEEK surface [8,25].

Fig. 3 shows the N and P concentrations of the PMPC-grafted PEEK as a function of the photo-irradiation time during polymerization at 0.25- and 0.50-mol/L MPC concentrations. The N and P concentrations increased with the photo-irradiation time. When the photo-irradiation time was shorter than 45 min, the N and P concentrations of the PMPC-grafted PEEK surface with a 0.50-mol/L MPC concentration were higher as compared with those with a 0.25-mol/L MPC concentration. The N and P concentration in the PMPC-grafted PEEK with both 0.25- and 0.50-mol/L MPC

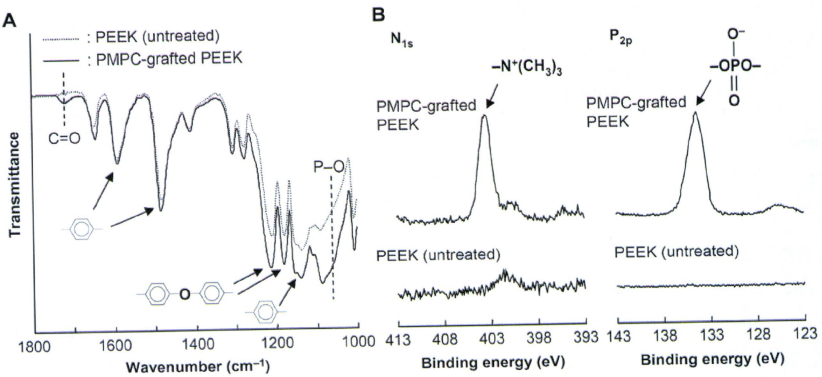

Fig. 2. FT-IR/ATR (A) and XPS (B) spectra of untreated and PMPC-grafted PEEK.

concentrations increased to 5.2 up to a photo-irradiation time of 90 min; those values were almost equivalent to the theoretical elemental composition (N = 5.3, P = 5.3) of PMPC. These results indicate that the PMPC layer fully covered the surface of the PEEK substrate.

Fig. 4 shows the cross-sectional TEM images of PMPC-grafted PEEK obtained with a 0.50-mol/L concentration and various photo-irradiation times as well as the PMPC-graft layer thickness determined by the TEM observations. With photo-irradiation times longer than 45 min, a uniform PMPC layer was clearly observed on the PEEK surface (Fig. 4(A)). The PMPC-graft layer thickness increased with the photo-irradiation time (Fig. 4(B)). In the case of both 0.25- and 0.50-mol/L MPC concentrations, when the photo-irradiation time was greater than 45 min, the PMPC-graft layer thicknesses became almost constant at 40 and 100, respectively.

Fig. 5 shows the physical properties of PMPC-graft layer on the PEEK surface as a function of the photo-irradiation time at MPC concentrations of 0.25 and 0.50 mol/L. The PMPC-graft extent of the PMPC-grafted PEEK with both 0.25- and 0.50-mol/L MPC concentration increased gradually with the photo-irradiation time (Fig. 5(A)). The PMPC-graft layer density of the PMPC-grafted PEEK with 0.25-mol/L MPC concentration increased proportionally to 2.3 g/cm^3 with the photo-irradiation time. In the case of PMPC-grafted PEEK obtained with 0.50-mol/L MPC concentration, the PMPC-graft layer density rapidly increased to 1.3 g/cm^3 up to a photo-irradiation time of 10 min; it then increased slowly to 2.2 g/cm^3 with an increase in the photo-irradiation time.

Fig. 6 shows the static-water contact angle of PMPC-grafted PEEK obtained with MPC concentrations of 0.25 and 0.50 mol/L as a function of the photo-irradiation time. The static-water contact angle of untreated PEEK was 90° and decreased markedly with an increase in the photo-irradiation time. When the photo-irradiation time was 90 min, the static-water contact angle of PMPC-grafted PEEK was the lowest value at <10°.

Fig. 7 shows the coefficient of dynamic friction of PMPC-grafted PEEK obtained with 0.25- and 0.50-mol/L MPC concentrations and various photo-irradiation times. For PMPC-grafted PEEK obtained with both 0.25- and 0.50-mol/L MPC concentrations, these coefficients of dynamic friction decreased markedly with an increase in photo-irradiation time. The PMPC-grafted PEEK obtained with 90 min photo-irradiation time was the lowest at <0.01, and exhibited approximately 95% reduction in their coefficients of dynamic friction when compared with the untreated PEEK.

Fig. 8 shows the amount of adsorbed BSA of PMPC-grafted PEEK as a function of the photo-irradiation time with MPC concentrations of 0.25 mol/L and 0.50 mol/L. The amount of adsorbed BSA of PMPC-grafted PEEK decreased remarkably with an increase in photo-irradiation time.

The mechanical properties of untreated PEEK and PMPC-grafted PEEK are summarized in Table 1. Tensile properties and flexural modulus did not differ significantly ($p > 0.05$) between untreated PEEK and PMPC-grafted PEEK. In contrast, there was a small but significant difference ($p < 0.05$) in the flexural strength and strain of untreated PEEK and PMPC-grafted PEEK examined in this study. However, both untreated PEEK and PMPC-grafted PEEK met the ASTM F2026 requirements [28].

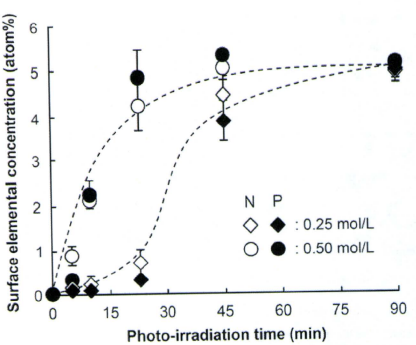

Fig. 3. Surface elemental concentration ($n = 5$) of PMPC-grafted PEEK as a function of the photo-irradiation time with MPC concentrations of 0.25 and 0.50 mol/L. Bar: Standard deviation.

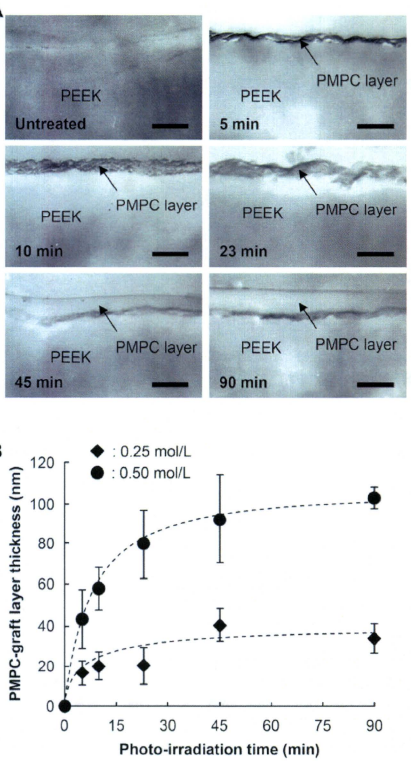

Fig. 4. Cross-section of the PMPC-grafted PEEK. (A) Cross-sectional TEM images of PMPC-grafted PEEK obtained with a MPC concentration of 0.5 mol/L and various photo-irradiation times. Bar: 100 nm. (B) PMPC-graft layer thickness ($n = 10$) determined by TEM observation. Bar: Standard deviation.

4. Discussion

In this study, we demonstrated the fabrication of a biocompatible and highly hydrophilic nanometer-scale-modified surface by PMPC-grafting onto the self-initiated PEEK surface using a photo-induced grafting-from polymerization reaction, i.e., "self-initiated surface graft polymerization." The following methods were employed in our study: (a) grafting from polymerization for the formation of a high-density graft polymer layer, (b) photo-induced polymerization in the absence of photo-initiators, and (c) using biocompatible hydrophilic macromolecules, which exhibited photo-reduction by H-abstraction of a BP unit in PEEK from an H-donor; this induced surface-initiated graft polymerization of the feed methacrylate-type monomer (i.e., MPC) on the PEEK surface, even in the absence of a photo-initiator such as BP. This report discusses the structure of the PMPC layer of PMPC-grafted PEEK in terms of the condition variability of self-initiated surface graft polymerization and its effects on antibiofouling and hydrophilicity.

It is important to control the graft layer thickness and density for optimizing several areas of applications, e.g., in adhesion, colloid stabilization, and lubrication. In Fig. 4, when the photo-irradiation time was greater than 45 min, the PMPC-graft layer thicknesses became almost constant. Moreover, at the same photo-irradiation time of 90 min, it was shown that the higher the monomer concentration, the thicker the graft layer obtained: the PMPC-graft layer thickness (approximately 100 nm) of the PMPC-grafted PEEK obtained with 0.50-mol/L MPC concentration was thicker than that (approximately 40 nm) with 0.25-mol/L MPC concentration. The phenomenon can be attributed to the fact that the graft layer thickness increases with monomer concentration. When the PMPC layer has a brush-like structure, the graft layer thickness may correlate with the molecular weight of the grafted PMPC. The high-density PMPC-graft layer on the PEEK surface is assumed to exhibit a brush-like structure [29,30]. It is generally well known that the reaction rate of radical polymerization is extremely high [31]. It was observed that the graft layer thickness (i.e., molecular weight of the graft polymer) was greatly dependent on the monomer concentration, but virtually independent of the photo-irradiation time. Thus, in this study, the length (molecular weight) of the PMPC-graft chains was assumed to be successfully controlled by the MPC concentration used for polymerization. This indicates that the length of the PMPC chain grafted on the PEEK surface increased with the MPC concentration during polymerization [32]. Additionally, a uniform PMPC layer was clearly observed on the surface of the PEEK substrate, and no cracks or delamination were observed at the PEEK substrate or the interface between the PMPC layer and PEEK substrate. These results indicate that the PMPC layer formed on the PEEK substrate is uniformly distributed over the substrate and is bound to the substrate by covalent C–C bonds.

On the other hand, the PMPC-graft layer density on the PEEK surface almost linearly increased to $>2.2\ g/cm^3$ with the photo-irradiation time, suggesting that the graft chain propagates steadily with increasing photo-irradiation time (Fig. 5(B)). In order to obtain the high-density PMPC-graft layer, the photo-irradiation time must be controlled. Further, interestingly, while using an MPC concentration of 0.50 mol/L, the rate of the increase in the PMPC-graft layer density was low with a photo-irradiation time above 10 min. The present self-initiated surface graft polymerization method is photo-induced by UV-irradiation onto the BP unit of PEEK surface. In this study, it is assumed that the UV-irradiation directly produces a high-concentration free radical, because this PEEK is a semi-crystalline structure (crystallinity, 30–40%) with a high-density BP unit in the surface. When the MPC concentration in a feed is also high, the self-initiated surface graft polymerization between the radicals on the PEEK surface and the MPC monomer occurs extremely rapidly in the reaction system, forming the high-density graft chain on the surface. Hence, diffusion of the MPC monomer onto the PEEK surface might be interfered by the high-density graft chain because of its high viscosity. When the monomers attached to the PEEK surface were subjected to UV-irradiation, radicals were freely formed on the PEEK surface in the early stage but not in the late stage of polymerization, probably because the high-density grafted polymer chains formed by then blocked the diffusion of the monomer to the PEEK surface. Therefore, it is supposed that the rate of increase in the PMPC-graft layer density changed due to the high concentration of free radicals and monomers.

The water-wettability of the PMPC-grafted PEEK surface is considerably greater than that of the untreated PEEK surface (Fig. 6), because of the presence of a nanometer-scaled PMPC layer (Fig. 4(A)): MPC is a highly hydrophilic compound, while PMPC is water-soluble. In Figs. 4–7, we observe that the dynamic coefficient

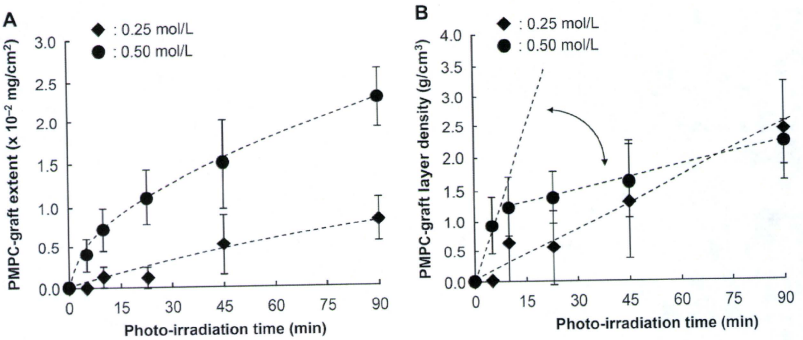

Fig. 5. Physical properties ($n = 5$) of PMPC-graft layer on PEEK surface as a function of the photo-irradiation time with MPC concentrations of 0.25 and 0.50 mol/L. (A) PMPC-graft extent by weighting, and (B) density calculated by (A) and mean PMPC-graft layer thickness of Fig. 4(B). Bar: Standard deviation.

of friction was greatly dependent on the water-wettability (static-water contact angle), but virtually independent of the structure (thickness and density) of the graft layer. A significant reduction in the static-water contact angle of the PMPC-grafted surface resulted in a substantial improvement in friction property. Fluid-film lubrication (or hydration lubrication) with the PMPC-grafted surface was achieved by the intermediate hydrated layer. It can be affirmed that this highly lubricated surface utilizing PMPC mimics the natural cartilage structure [33]. When the PEEK surface is modified by PMPC-grafting, the grafted PMPC causes a significant reduction in sliding friction between the graft surfaces because the thin water films that are formed act as extremely efficient lubricants. The water-lubrication systems utilizing PMPC suppress direct contact of the counter-bearing face with the PEEK substrate in order to reduce the frictional force. Thus, the PMPC-graft layer is expected to significantly increase the durability of the bearing biomaterials. On the other hand, when the photo-irradiation time was shorter than 23 min, the decrease in the static-water contact angle of the PMPC-grafted PEEK surface with a 0.25-mol/L MPC concentration was only slight. It was thought that the surface phenomenon was caused by the pinacolization reaction, because the static-water contact angle of the UV-irradiated PEEK surface without monomer was decreased to approximately 80° (data not shown).

The fabrication of surfaces that exhibit anti-protein adsorption and/or cell adhesion has been one of goals of surface engineering for medical devices. The adsorption of the BSA on the PMPC-grafted PEEK surface decreased to 10% ($p < 0.001$) with an increase in photo-irradiation time, as shown in Fig. 8, as compared to that in untreated PEEK. It is shown that the extent of protein rejection is related to the PMPC-graft extent (Figs. 5(A) and 8). Extensive grafting gives rise not only to an increase in the thickness of graft layer but also to an increase in the volume fraction (i.e., density) of graft segments in the layer. Therefore, it was thought that these characteristics of thickness and density of the PMPC-graft layer had a significant influence on protein adsorption. The mechanism of protein adsorption resistance on the PMPC-grafted surface is

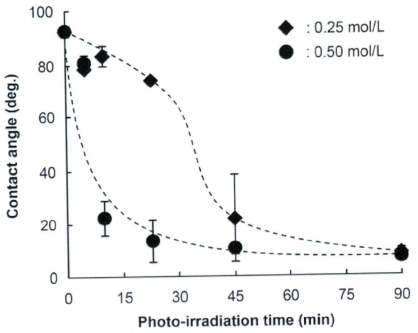

Fig. 6. Static-water contact angle ($n = 15$) of PMPC-grafted PEEK as a function of the photo-irradiation time with MPC concentrations of 0.25 and 0.50 mol/L. Bar: Standard deviation.

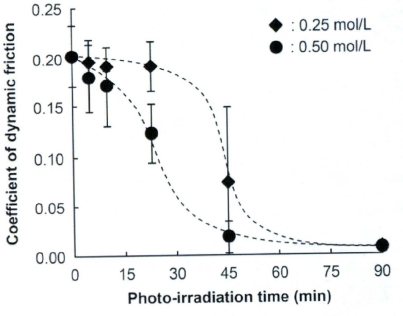

Fig. 7. Coefficient of dynamic friction ($n = 5$) of PMPC-grafted PEEK as a function of the photo-irradiation time with MPC concentrations of 0.25 and 0.50 mol/L. Bar: Standard deviation.

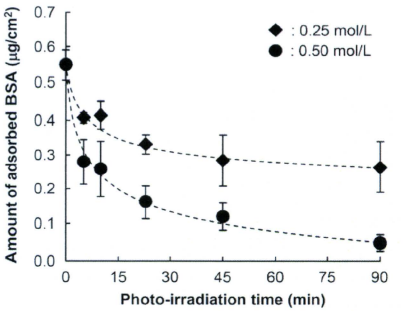

Fig. 8. Amount of adsorbed BSA ($n = 3$) of PMPC-grafted PEEK as a function of the photo-irradiation time with MPC concentrations of 0.25 and 0.50 mol/L. Bar: Standard deviation.

hypothesized as follows: the protein adsorption resistance attributed to the water-fluid film and hydration layer was due to water and hydrophilic macromolecules with volume exclusion effects. The presence of the water-fluid film and hydration layer is responsible for the easy detachment of proteins and the prevention of conformational changes in the adsorbed proteins [34]. These observations are consistent with the results of the static-water-contact angle measurements, cross-sectional TEM observations, and PMPC-graft layer weighting of the PEEK whose surface was modified by PMPC-grafting. These results imply that the PMPC-grafted PEEK surface is biocompatible in terms of tissue and blood compatibility, because MPC polymer-modified surfaces are known to exhibit *in vivo* antibiofouling [16,20,23,24].

As shown in Table 1, the mechanical properties of the PEEK are unchanged even after PMPC-grafting. This indicates that the photo-induced radical graft polymerization proceeds only on the surface of the PEEK substrate, while the properties of the substrate remain unchanged. Retention of the properties of the PEEK substrate is very important in clinical use, because the biomaterials used in implants act not only as surface-functional materials but also as structural materials *in vivo*.

The design of a well-characterized surface is a considerably important and difficult task. The photo-induced graft polymerization in the absence of photo-initiators of this study, i.e., "self-initiated surface graft polymerization" successfully prepared the surface with controlled graft layer thickness and density. This simple self-initiated surface graft polymerization would be highly suitable for industrial applications [35,36] as well as the development of medical devices [2–7]. The synthesis of a self-initiated biocompatible polymer having unique properties such as anti-protein adsorption and wettability by the photo-induced grafting-from polymerization reaction is a novel phenomenon in the field of biomaterials and bioengineering sciences, and the fabrication of the PMPC-grafted PEEK surface can result in the development of next-generation multifunctional biomaterials.

Table 1
Mechanical properties ($n = 10$) of untreated and PMPC-grafted PEEK.

Test method	Property	PEEK (untreated)	PMPC-grafted PEEK	*t*-Test
Tensile test	Yield strength (MPa)	109.4 (0.4)[a]	109.9 (0.6)	N.S.
	Ultimate strength (MPa)	71.5 (1.5)	71.7 (1.7)	N.S.
	Elongation (%)	24.0 (9.5)	24.4 (9.0)	N.S.
Flexural test	Ultimate strength (MPa)	168.9 (0.6)	173.7 (1.8)	<0.05
	Ultimate strain (%)	6.4 (0.1)	6.7 (0.2)	<0.05
	Modulus (GPa)	3.9 (0.0)	3.9 (0.0)	N.S.

[a] The standard deviations are shown in parenthesis.

5. Conclusions

A biocompatible and highly hydrophilic nanometer-scale-modified surface was successfully fabricated on the PEEK substrate by the photo-induced graft polymerization of PMPC in the absence of photo-initiators, i.e., "self-initiated surface graft polymerization." Since MPC is a highly hydrophilic compound, the water wettability and lubricity of the PMPC-grafted PEEK surface were greater than that of the untreated PEEK surface due to the formation of a PMPC nanometer-scale layer. In addition, the amount of BSA adsorbed on the PMPC-grafted PEEK surface considerably decreased compared to that in the case of untreated PEEK. The density and thickness of the grafting layer could be controlled by the photo-irradiation time and monomer concentration.

References

[1] Williams DF, McNamara A, Turner RM. Potential of polyetheretherketone (PEEK) and carbon-fibre-reinforced PEEK in medical applications. J Mater Sci Lett 1987;6:188–90.
[2] Kurtz SM, Devine JN. PEEK biomaterials in trauma, orthopedic, and spinal implants. Biomaterials 2007;28(32):4845–69.
[3] Wang A, Lin R, Stark C, Dumbleton JH. Suitability and limitations of carbon fiber reinforced PEEK composites as bearing surfaces for total joint replacements. Wear 1999;225–229:724–7.
[4] Joyce TJ, Rieker C, Unsworth A. Comparative in vitro wear testing of PEEK and UHMWPE capped metacarpophalangeal prostheses. Biomed Mater Eng 2006;16(1):1–10.
[5] Latif AM, Mehats A, Elcocks M, Rushton N, Field RE, Jones E. Pre-clinical studies to validate the MITCH PCR Cup: a flexible and anatomically shaped acetabular component with novel bearing characteristics. J Mater Sci Mater Med 2008;19(4):1729–36.
[6] Yu S, Hariram KP, Kumar R, Cheang P, Aik KK. In vitro apatite formation and its growth kinetics on hydroxyapatite/polyetheretherketone biocomposites. Biomaterials 2005;26(15):2343–52.
[7] Fan JP, Tsui CP, Tang CY, Chow CL. Influence of interphase layer on the overall elasto-plastic behaviors of HA/PEEK biocomposite. Biomaterials 2004;25(23):5363–73.
[8] Kyomoto M, Ishihara K. Self-initiated surface graft polymerization of 2-methacryloyloxyethyl phosphorylcholine on poly(ether-ether-ketone) by photo-irradiation. ACS Appl Mater Interfaces 2009;1(3):537–42.
[9] Giancaterina S, Rossi A, Rivaton A, Gardette JL. Photochemical evolution of poly(ether ether ketone). Polym Degrad Stab 2000;68(1):133–44.
[10] Wang H, Brown HR, Li Z. Aliphatic ketones/water/alcohol as a new photo-initiating system for the photografting of methacrylic acid onto high-density polyethylene. Polymer 2007;48(4):939–48.
[11] Yang W, Rånby B. Photoinitiation performance of some ketones in the LDPE–acrylic acid surface photografting system. Eur Polym J 1999;35(8):1557–68.
[12] Qiu C, Nguyen QT, Ping Z. Surface modification of cardo polyetherketone ultrafiltration membrane by photo-grafted copolymers to obtain nano-filtration membranes. J Membr Sci 2007;295(1–2):88–94.
[13] Nguyen HX, Ishida H. Molecular analysis of the melting behaviour of poly(aryl-ether-ether-ketone). Polymer 1986;27(9):1400–5.
[14] Cole KC, Casella IG. Fourier transform infrared spectroscopic study of thermal degradation in films of poly(etheretherketone). Thermochim Acta 1992;211:209–28.
[15] Qiu KY, Si K. Grafting reaction of macromolecules with pendant amino groups via photoinitiation with benzophenone. Macromol Chem Phys 1996;197:2403–13.
[16] Moro T, Takatori Y, Ishihara K, Konno T, Takigawa Y, Matsushita T, et al. Surface grafting of artificial joints with a biocompatible polymer for preventing peri-prosthetic osteolysis. Nat Mater 2004;3:829–37.
[17] Moro T, Takatori Y, Ishihara K, Nakamura K, Kawaguchi H. 2006 Frank Stinchfield Award: grafting of biocompatible polymer for longevity of artificial hip joints. Clin Orthop Relat Res 2006;453:58–63.
[18] Moro T, Kawaguchi H, Ishihara K, Kyomoto M, Karita T, Ito H, et al. Wear resistance of artificial hip joints with poly(2-methacryloyloxyethyl phosphorylcholine) grafted polyethylene: comparisons with the effect of polyethylene cross-linking and ceramic femoral heads. Biomaterials 2009;30(16):2995–3001.
[19] Sibarani J, Takai M, Ishihara K. Surface modification on microfluidic devices with 2-methacryloyloxyethyl phosphorylcholine polymers for reducing unfavorable protein adsorption. Colloids Surf B Biointerfaces 2007;54(1):88–93.

[20] Ueda T, Oshida H, Kurita K, Ishihara K, Nakabayashi N. Preparation of 2-methacryloyloxyethyl phosphorylcholine copolymers with alkyl methacrylates and their blood compatibility. Polym J 1992;24(11):1259–69.
[21] Konno T, Ishihara K. Temporal and spatially controllable cell encapsulation using a water-soluble phospholipid polymer with phenylboronic acid moiety. Biomaterials 2007;28(10):1770–7.
[22] Xu Y, Takai M, Konno T, Ishihara K. Microfluidic flow control on charged phospholipid polymer interface. Lab Chip 2007;7(2):199–206.
[23] Snyder TA, Tsukui H, Kihara S, Akimoto T, Litwak KN, Kameneva MV, et al. Preclinical biocompatibility assessment of the EVAHEART ventricular assist device: coating comparison and platelet activation. J Biomed Mater Res A 2007;81(1):85–92.
[24] Ueda H, Watanabe J, Konno T, Takai M, Saito A, Ishihara K. Asymmetrically functional surface properties on biocompatible phospholipid polymer membrane for bioartificial kidney. J Biomed Mater Res A 2006;77(1):19–27.
[25] Kyomoto M, Moro T, Konno T, Takadama H, Yamawaki N, Kawaguchi H, et al. Enhanced wear resistance of modified cross-linked polyethylene by grafting with poly(2-methacryloyloxyethyl phosphorylcholine). J Biomed Mater Res A 2007;82(1):10–7.
[26] Ishihara K, Ueda T, Nakabayashi N. Preparation of phospholipid polymers and their properties as polymer hydrogel membranes. Polym J 1990;22(5):355–60.
[27] He D, Susanto H, Ulbricht M. Photo-irradiation for preparation, modification and stimulation of polymeric membranes. Prog Polym Sci 2009;34:62–98.
[28] ASTM F2026–02: Standard specification for polyetheretherketone (PEEK) polymers for surgical implant applications. In: Arendt SA, Bailey SJ, editors. Annual book of ASTM standards, vol. 13, 2004.
[29] Kyomoto M, Moro T, Iwasaki Y, Miyaji F, Kawaguchi H, Takatori Y, et al. Superlubricious surface mimicking articular cartilage by grafting poly (2-methacryloyloxyethyl phosphorylcholine) on orthopaedic metal bearings. J Biomed Mater Res A 2009;91(3):730–41.
[30] Matsuda T, Kaneko M, Ge S. Quasi-living surface graft polymerization with phosphorylcholine group(s) at the terminal end. Biomaterials 2003;24: 4507–15.
[31] Braunecker WA, Matyjaszewski K. Controlled/living radical polymerization: features, developments, and perspectives. Prog Polym Sci 2007;32(1): 93–146.
[32] Kyomoto M, Moro T, Miyaji F, Hashimoto M, Kawaguchi H, Takatori Y, et al. Effect of 2-methacryloyloxyethyl phosphorylcholine concentration on photo-induced graft polymerization of polyethylene in reducing the wear of orthopaedic bearing surface. J Biomed Mater Res A 2008;86(2):439–47.
[33] Ishikawa Y, Hiratsuka K, Sasada T. Role of water in the lubrication of hydrogel. Wear 2006;261:500–4.
[34] Kyomoto M, Moro T, Miyaji F, Hashimoto M, Kawaguchi H, Takatori Y, et al. Effects of mobility/immobility of surface modification by 2-methacryloyloxyethyl phosphorylcholine polymer on the durability of polyethylene for artificial joints. J Biomed Mater Res A 2009;90(2):362–71.
[35] Hasegawa S, Suzuki Y, Maekawa Y. Preparation of poly(ether ether ketone)-based polymer electrolytes for fuel cell membranes using grafting technique. Radiat Phys Chem 2008;77:617–21.
[36] Chen J, Asano M, Maekawa Y, Yoshida M. Fuel cell performance of polyetheretherketone-based polymer electrolyte membranes prepared by a two-step grafting method. J Membr Sci 2008;319:1–4.

Biomaterials 31 (2010) 2380–2387

Contents lists available at ScienceDirect

Biomaterials

journal homepage: www.elsevier.com/locate/biomaterials

Cell-penetrating macromolecules: Direct penetration of amphipathic phospholipid polymers across plasma membrane of living cells

Tatsuro Goda [a,c,1], Yusuke Goto [a,c], Kazuhiko Ishihara [a,b,c,*]

[a] Department of Materials Engineering, School of Engineering, The University of Tokyo, 7-3-1 Hongo, Bunkyo, Tokyo 113-8656, Japan
[b] Department of Bioengineering, School of Engineering, The University of Tokyo, 7-3-1 Hongo, Bunkyo, Tokyo 113-8656, Japan
[c] Center for NanoBio Integration, The University of Tokyo, 7-3-1 Hongo, Bunkyo, Tokyo 113-8656, Japan

ARTICLE INFO

Article history:
Received 9 November 2009
Accepted 26 November 2009
Available online 9 December 2009

Keywords:
Phospholipid polymer
Amphiphilicity
Non-endocytosis
Drug delivery
Molecular imaging

ABSTRACT

Nanoscaled materials are normally engulfed in endosomes by energy-dependent endocytosis and fail to access the cytosolic cell machinery. Although some biomolecules may penetrate non-endocytically or fuse with plasma membranes without overt membrane disruption, to date no synthetic macromolecule of comparable size has been shown to exhibit this property. Here, we discovered mechanism of direct cell membrane penetration using synthetic phospholipid polymers. These water-soluble amphiphilic phospholipid polymers enter the cytoplasm of living mammalian cells *in vitro* within a few minutes without overt bilayer disruption even under conditions where energy-dependent endocytic uptakes are blocked. Furthermore, targeted cytosolic distribution to cell organelles was achieved by selecting specific fluorescent tags to the polymers. Thus, the phospholipid polymers can provide a new way of thinking about access to the cellular interior, namely direct membrane penetration.

© 2009 Elsevier Ltd. All rights reserved.

1. Introduction

Nanomaterials are of great interest for their potential biomedical applications as imaging tools [1,2] therapeutic agents [3], and drug/gene delivery carriers [4,5]. However, the plasma membrane of eukaryotic cells constitutes a highly selective permeability barrier that prevents the passage of nanomaterials, allowing only small, uncharged molecules to gain access to the cell interior. Thus, translocation of nanomaterials across plasma membranes is currently one of the most actively researched topics in nanobiology. The most common mechanism of cellular uptake for nanomaterials is endocytosis, an energy-dependent process in which the nanomaterial is trapped within endosomes that carry ingested material into the cellular interior while the engulfed materials do not gain access to the cytosol [6]. Cationically charged nanomaterials, such as dendrimers [7], quantum dots [8], and polymeric micelles [9], can pass through anionic plasma membranes by causing transient pore formation, a process that is also associated with cytotoxicity. Alternatively, nanoparticles coupled with exogenous cell-penetrating peptides (CPPs) have been designed to explicitly disrupt the endolysosomal membrane, thereby facilitating entry into the cytosol [10,11]. CPP-conjugated nanomaterials may be capable of directly penetrating the membrane without overt lipid bilayer disruption. To the best of our knowledge, however, no synthetic macromolecules larger than a few nanometers in size can penetrate directly through the plasma membrane without disturbing the integrity of the biological barriers.

Phospholipid molecules play a crucial role in determining the composition of the cytosol by forming a bilayer structure with barrier properties and mass transport function. In addition, they form a bio-inert surface in the cell membrane that facilitates highly efficient, selective, and specific biological reactions. By mimicking the chemical functionality as well as the molecular structure of phospholipids in the plasma membrane, we have synthesized phospholipid polymers comprising 2-methacryloyloxyethyl phosphorylcholine (MPC) as a polar group and *n*-butyl methacrylate (BMA) as a hydrophobic part [12]. The poly(MPC-co-BMA) (PMB), which forms nanoassemblies (polymeric aggregates) or nanoparticles in aqueous media depending on the degree of hydrophobicity and molecular weight of the polymers, has considerable potential for therapeutic nanomaterials [13]. Previously, a PMB carrying an antineoplastic drug was demonstrated to exhibit antitumor effects on cancer cells without cytotoxicity both *in vitro* and *in vivo* [14–16]; however, the mechanism whereby the drug in the PMB was delivered across the plasma membrane of cells remains

* Corresponding author. Department of Materials Engineering, School of Engineering, The University of Tokyo, 7-3-1 Hongo, Bunkyo, Tokyo 113-8656, Japan. Tel.: +81 3 5841 7124; fax: +81 3 5841 8647.
E-mail address: ishihara@mpc.t.u-tokyo.ac.jp (K. Ishihara).
[1] Current address: Biomaterials Center, National Institute for Materials Science, 1-1 Namiki, Tsukuba, Ibaraki 305-0044, Japan.

0142-9612/$ – see front matter © 2009 Elsevier Ltd. All rights reserved.
doi:10.1016/j.biomaterials.2009.11.095

poorly understood. In this study, we discovered direct penetration mechanism across the plasma membrane of living mammalian cells using fluorescence-tagged PMBs.

2. Materials and methods

2.1. Materials

MPC, which was synthesized as previously described [17], was purchased from NOF (Tokyo, Japan). The commercially available reagents *n*-butyl methacrylate (BMA; Nacalai Tesque, Tokyo, Japan), methacryloxyethyl thiocarbonyl rhodamine B (MTR; Polysciences, PA, USA), *o*-methacryloyl Hoechst 33258 (Polysciences), fluorescein *o*-methacrylate (Polysciences), 1-pyrenylmethyl methacrylate (Polysciences), t-butyl peroxyneodecanoate (Perbutyl-ND; NOF), and 2,2′-azobisisobutyronitrile (AIBN; Kanto Chemical Co., Tokyo, Japan) were of extra pure grade and used without further purification. Unless stated otherwise, all the other materials were purchased from commercial sources and used as received.

2.2. Synthesis of fluorescent polymers

The poly(MPC-*co*-BMA) with covalent labeling of rhodamine B (rhoPMB) was synthesized using a free radical polymerization technique with Perbutyl-ND as an initiator. For rhoPMB30 synthesis, MPC (2.66 g, 9.00 mmol), BMA (2.99 g, 21.0 mmol), and MTR (20.5 mg, 30.0 μmol) were dissolved in ethanol (30.0 mL) and argon gas was bubbled through the resulting solution for 30 min in order to remove dissolved oxygen. Perbutyl-ND (70 wt% in hydrocarbons, 0.367 g, 1.05 mmol) was then added to the solution and the temperature was elevated to 60 °C for 12 h to induce polymerization. Thereafter, the polymer was reprecipitated twice in diethylether/chloroform (7/3 v/v). The polymer was then dialyzed against water through a regenerative cellulose membrane (MWCO, 3.5 kDa) for 7 days, and subsequently ultrafiltrated in methanol/water (7/3 v/v) for 7 days (MWCO, 5.0 kDa) to remove unreacted monomers and absorbed dyes. rhoPMB50, rhoPMB80, and rhodamine B-labeled poly(MPC) (rhoPMPC; MPC/MTR = 100/0.1 mol/mol) were synthesized using the same method. Hoechst 33258-tagged PMB30 (hoechstPMB30) and FITC-tagged PMB30 (fitcPMB30) were synthesized using the same method used to synthesize rhoPMB30, but using *o*-methacryloyl Hoechst 33258 and fluorescein *o*-methacrylate, respectively, instead of MTR. High molecular weight rhoPMB polymers were synthesized using a free radical polymerization technique with AIBN (4.90 mg, 30.0 μmol) instead of perbutyl-ND as an initiator, and were purified using the same method described above. The high molecular weight polymers were dialyzed against water through a regenerative cellulose membrane (MWCO, 50 kDa).

2.3. Cell culture

The human Caucasian hepatocyte carcinoma (HepG2) cell line (RIKEN Bio-Resource Center, Ibaraki, Japan) was seeded on tissue culture polystyrene (1.0×10^4 cells/cm^2) in DMEM supplemented with 10% fetal bovine serum (FBS, Gibco), and penicillin/streptomycin (100 μg/mL, Gibco) at 37 °C in 5% CO_2. Sub-confluent cultures (70–80%) were passaged using 0.25% trypsin/EDTA at 37 °C in 5% CO_2. HeLa cells (RIKEN BioResource Center) were passaged at sub-confluency in DMEM containing 10% FBS.

2.4. Cellular uptake of fluorescent-labeled polymers

Cells were seeded into glass-bottom dishes (0.12–0.17 mm thick; Matsunami, Osaka, Japan) at $5.0–6.0 \times 10^4$ cells/mL in 1.0 mL of culture medium and grown for 1 day before incubation with the fluorescent polymers. The cells were then rinsed 3 times with DPBS. The medium was subsequently exchanged with fresh warm serum-free or serum-containing (10% FBS) DMEM and fluorescent polymers were added from a concentrated stock solution in DMEM at a final concentration of 1.0 mg mL^{-1}. Cells were incubated with fluorescence-tagged polymer at 37 °C in 5% CO_2 for the desired length of time. After incubation with the polymer, the cells were rinsed 3 times with DPBS and placed in 1.0 mL of DMEM for live cell imaging. Staining of cells under conditions of energy depletion was performed by incubating the cells with 3.0 mM sodium azide and 50 mM 2-deoxy-D-glucose in DPBS (ATP depletion solution). Cells were pre-incubated in ATP depletion solution at 37 °C for 30 min and then incubated with 1.0 mg mL^{-1} fluorescent polymers in ATP depletion medium at 37 °C in 5% CO_2. The cells were then washed 3 times with DPBS and placed in 1.0 mL of DMEM. Staining under conditions inhibitory to the mechanism of active uptake by cells was performed by incubating at 4 °C. Cultured cells were washed 3 times with DPBS and precooled in serum-free DMEM at 4 °C for 30 min. The cells were then incubated in serum-free DMEM with 1.0 mg mL^{-1} fluorescence-tagged polymer at 4 °C. Thereafter, the cells were rinsed 3 times with DPBS and placed in 1.0 mL of serum-free DMEM.

2.5. Confocal fluorescent microscopy studies

The polymers in living cells were imaged using an LSM-510 Meta confocal microscope (Carl Zeiss, Oberkochen, Germany) equipped with a 63× oil-immersion objective lens with a numerical aperture of 1.4 with respect to the beam waist. Confocal-DIC images were obtained by excitation with a 633-nm HeNe laser line. Fluorescent probes in Hoechst 33258-, FITC-, and rhodamine B-tagged polymers in the cells were excited with a 405-nm line (selected by an extra 405 ± 10 nm interference-based laser cleanup filter) of a blue diode laser, a 488-nm line of an Ar laser, and a 543-nm line of a HeNe laser, respectively. The excitation light was directed to the sample by a dichroic mirror (DC; HFT 405, 488, and 543, respectively). Each fluorescent light was sent through the DC and a long-pass LP 420 nm, band-pass BP 520–550 nm, and LP 560 nm emission filter to an analog photomultiplier tube used for detection. The detector gain was set to 650–850 units in the Zeiss software. Dark signal contributions to the images were effectively zeroed out by setting the proper detection offset value as provided in the Zeiss software. The image size was typically set to 512 × 512 or 1024 × 1024 pixels. Multi-stained cells were imaged using multi-track mode for the prevention of cross-talk. The full cellular thickness (approximately 11 μm) was scanned with the confocal microscope in 1.4-μm steps. Confocal Z-section scanning for imaging of the nucleus was conducted in 0.4-μm steps. The internalization of rhodamine B-tagged polymers into living cells was monitored by time-lapse imaging every 30 s up to 30 min at 37 °C. After rinsing 3 times with DPBS, cultured cells were placed in fresh warm serum-free DMEM and the glass-bottom dish was placed on a temperature control module under a 63× oil lens. Time-lapse imaging was started just after the fluorescent polymer was added from a concentrated stock solution in DMEM at a final concentration of 1.0 mg mL^{-1}.

2.6. Fluorescence correlation spectroscopy (FCS) studies

Scanning measurements were performed using an LSM 510 Meta microscope equipped with a ConfoCor 3 unit for FCS (Carl Zeiss). MTR and rhodamine B-tagged polymer were excited at 543 nm by the built-in HeNe laser, focused onto the sample by a 40× water-immersion objective lens (C-Apochromat) with a numerical aperture of 1.2 relative to the beam waist with $1/e^2$ radius $\omega_{xy} = 0.2$ μm. The pinhole in front of the avalanche photodiode was set to 78 μm. Fluorescence was detected by an avalanche photodiode in the ConfoCor unit. To select the detected spectral range, an LP 560-nm filter was used for the measurements. The fluorescence temporal signal was recorded, and the autocorrelation function $G(t)$ was calculated using the internal correlator. Curve fittings were carried out using ConfoCor, with a triplet state identified in the fitting, and with two-dimensional fitting. The waist radius (ω_1) of the 543-nm laser lines was set at 0.20 μm on the basis of the known diffusion coefficient of rhodamine B in solution ($D = 28 \times 10^{-9}$ m^2/s). The effective diffusion coefficients of the fluorescent-tagged polymer (D) were determined using the calibrated beam waist and the diffusion time obtained from the autocorrelation curve via the equation $D = \omega_1^2/4\tau_D$, where τ_D is the diffusion time. The temperature dependence of the diffusion coefficient can be written in the form of the Stokes–Einstein equation, $R_H = k_B T/6\pi\eta D$, where R_H denotes the hydrodynamic radius, k_B Boltzmann's constant, T the absolute temperature, and η the solution viscosity. The autocorrelation curve was generated from 30 × 15-s data collections.

2.7. Subcellular distribution of the fluorescent polymers

HepG2 cells were pre-incubated with 100 nM of MitoTracker Green FM (Molecular Probes), which is a specific fluorescence dye for mitochondria, in DMEM containing 10% FBS for 24 h at 37 °C in 5% CO_2. After rinsing 3 times with DPBS, the stained cells were incubated in serum-free DMEM containing rhoPMB (1.0 mg mL^{-1}) at 37 °C in 5% CO_2 for 30 min. The cells were then rinsed 3 times with DPBS and placed in 1.0 mL of DMEM for imaging using an LSM 510 Meta confocal microscope operating in multi-track mode. MitoTracker was excited with a 488-nm line and imaged through band-pass BP 520–550-nm emission filter to the PMT.

2.8. Flow cytometry studies

HepG2 cells (5.0×10^5) were seeded in 6-well culture plates and grown overnight in DMEM containing 10% FBS at 37 °C in 5% CO_2. After rinsing 3 times with DPBS, the cells were incubated with fluorescence-tagged polymers under the desired conditions. Thereafter, the cells were rinsed 3 times with DPBS and treated with trypsin/EDTA. The cells were then suspended in DMEM containing 10% FBS and analyzed immediately using an EPICS XL flow cytometer (Beckman Coulter, CA, USA) operating at 488-nm excitation and with either FL-2 or FL-3 emission filters. For the measurement of release of the fluorescence-tagged polymer from the cells, the suspension was incubated for 0–180 min at room temperature before flow cytometric analysis. A minimum of 1.0×10^4 cells were analyzed from each sample with florescence intensity.

2.9. Calcein-AM staining

Calcein-AM (10 μM in DPBS, Invitrogen) was pre-incubated with cells for 30 min in serum-containing DMEM (final concentration: 100 nM). Cells were then rinsed 3

times with DPBS. The medium was replaced with warm serum-free DMEM and rhodamine B-tagged polymers were added to a final concentration of 1.0 mg mL^{-1} for 30 min, before washing and measurement of calcein intensity by confocal microscopy and flow cytometry. As a control experiment, Lipofectin (final concentration: 10 μg mL^{-1}; Invitrogen) and Tween 20 (final concentration: 1.0 mg mL^{-1}, Aldrich) were used.

2.10. WST-8 assay

Assessment of the viability of cells after incubation with polymers for 24 h was carried out using a WST-8 assay (Dojindo, Tokyo, Japan), which is based on the cleavage of the tetrazolium salt to formazan by cellular mitochondrial dehydrogenase. Cells were seeded into 96-well plates at 1.0×10^4 cells/well in 100 μL of serum-containing DMEM. After preincubation for 3 h, polymers without fluorescence (10 μL) were added to the medium (final concentration: 1.0 mg mL^{-1}). Polymers in culture medium were incubated with cells for 21 h at 37 °C in 5% CO_2. Thereafter, 10 μL of WST-8 reagent was added to all cell culture medium and incubation was continued for a further 3 h (total 24 h). At the end of the incubation period, the microplates were read at 450 nm in an Appliskan microplate reader (ThermoFisher Scientific, MA, USA). A total of 110 μL of serum-containing DMEM with cells and 110 μL of serum-containing DMEM were used as the control and background, respectively. The average background absorbance from background control wells was subtracted from the sample data. The values for each sample were in the linear region of the standard curve of the WST-8 assay. Data are expressed as the means and SE ($n = 8$).

2.11. LDH release assay

Damage to cell membranes after incubation with polymers for 24 h was evaluated using a lactate dehydrogenase (LDH) assay kit (Wako, Osaka, Japan). Cells were seeded into 96-well plates at 1.0×10^4 cells/well in 100 μL of serum-containing DMEM. After preincubation for 3 h, polymers without fluorescence (10 μL) were added to the medium (final concentration: 1.0 mg mL^{-1}). Polymers in culture medium were incubated with cells for 24 h at 37 °C in 5% CO_2. Thereafter, 50 μL of cell-free supernatant was assayed using an LDH reagent kit according to the manufacturer's instructions. Absorbance at 560 nm was measured using an Appliskan microplate reader.

3. Results

We synthesized the rhoPMBs of approximately the same molecular weight but with different amphipathic natures, achieved by varying the MPC/BMA compositions (Table 1). The molar compositions determined by ^{1}H NMR (Fig. S1) approximately corresponded to their feed compositions. The rhoPMBs had hydrodynamic size of ca. 10 nm (Fig. S2). Importantly, zeta potential was nearly 0 mV. The fluorescence quantum yield of rhoPMB80 and rhoPMPC was slightly lower than that of rhoPMB30 and rhoPMB50 (Fig. S3); consequently, the fluorescence intensities of the former were compensated for during quantitative analysis. Covalent immobilization of rhodamine B on the polymers was confirmed by gel permeation chromatography (GPC) (Fig. S4). The GPC measurements also proved removal of the unreacted monomers and physically adsorbed dyes from the fluorescence-tagged polymers.

We used HepG2 (a human hepatocellular liver carcinoma cell line) cells because they are rich in mitochondria that can be easily visualized by confocal microscopy or studied by flow cytometry. In order to avoid potential artifacts caused by cell fixation, live cells were imaged under controlled temperature conditions. When rhoPMB30 was incubated with HepG2, it was observed to enter cells very rapidly and the fluorescence intensity continued to increase by real-time observation with confocal microscopy (Fig. 1a). Because endocytosis, including pinocytosis and phagocytosis, enables cells to internalize nanomaterials or small volumes of fluid that have no interaction with the plasma membrane into intracellular vesicles, we conducted internalization experiments in serum-free medium at 4 °C and under conditions of ATP depletion by incubating cells in 3.0 mM sodium azide and 50 mM 2-deoxy-D-glucose in DPBS at 37 °C. Under these conditions, active uptake by the cells is inhibited due to a deficiency in ATP. Surprisingly, substantial amount of rhoPMB30 was internalized even at 4 °C or in ATP depletion solution at 37 °C determined using confocal microscopy (Fig. 1b,c). We compared the fluorescence intensity of cells quantitatively using flow cytometry. The fluorescence intensity of cells incubated in ATP depletion solution reached the same level as that of cells in serum-free medium (Fig. 1d). A substantial level of fluorescence intensity compared with autofluorescence in cells incubated in serum-free medium at 4 °C was also confirmed. The observation that at least 50% of the uptake of rhoPMB30 into the cytosol occurred under conditions where endocytic processes were blocked suggests that the polymer is internalized in a non-endocytic manner. Interestingly, internalized rhoPMBs were able to escape from the cytoplasm when cells were incubated in polymer-free medium (Fig. S5). Although trends in polymer uptake and intracellular distribution were qualitatively similar in serum-free and serum-containing media, the comparable inhibition of cellular uptake of rhoPMB30 in serum-containing medium (Fig. 1d) presumably reflects binding to serum proteins [18]. Whether the fluorescent dyes located in the cytosol indicate the positions of rhoPMBs or simply fluorescent dye that has been enzymatically cleaved from the polymer was confirmed by relaxation modes of the fluorescent dyes in the cytosol using fluorescence correlation spectroscopy (FCS) [19]. FCS results showed slower translational diffusion of rhoPMB30 ($D_{\mathrm{rhoPMB30}} = 30\ \mu m^2/s$) than from methacryloxyethyl thiocarbonyl rhodamine B (MTR, $D_{\mathrm{MTR}} = 220\ \mu m^2/s$) (Fig. 1e, Table 2). The results clearly indicate cytosolic entry of rhoPMB30 without cleavage of rhodamine B from the polymer. Further, we observed direct penetration of water-soluble rhoPMBs with higher weight-average molecular weight (M_w) of up to 4.0×10^6 (Table S1, Fig. S6). Thus, direct penetration of rhoPMBs is seemingly independent of their M_w.

The effects of MPC/BMA ratio (*i.e.*, amphipathicity) of rhoPMBs on direct penetration were investigated. Intense rhodamine B levels in the cytoplasm after incubation with rhoPMBs for 30 min were commonly observed under conditions where endocytic uptake was facilitated or blocked using confocal microscopy (Fig. 2a, b). Quantitative comparison by flow cytometry revealed that there was no clear relationship between the MPC/BMA ratios of the polymers and fluorescence intensities of stained cells (Fig. 2c) In contrast,

Table 1
Physical and chemical properties of the rhodamine B-tagged random copolymers used in this study.

Fluorescent polymers	MPC/BMA composition[a], mol/mol	M_N[b], kDa	M_W[b], kDa	Hydrodynamic size[c], nm (PI)	ζ-potential[d], mV	Fluorescence quantum yield
rhoPMB30	29/71	7.3	24.0	9.5 (0.275)	4.1 ± 2.1	0.625
rhoPMB50	45/55	9.2	29.0	10.0 (0.224)	4.5 ± 2.1	0.619
rhoPMB80	71/29	15.9	41.1	12.1 (0.206)	2.2 ± 3.6	0.491
rhoPMPC	MPC 100%	51.6	159	12.6 (0.635)	0.4 ± 2.1	0.462

[a] MPC; 2-methacryloyloxyethyl phosphorylcholine, BMA; *n*-butyl methacrylate. Determined from ^{1}H NMR.
[b] Number-average (M_N) and weight-average (M_w) molecular weights measured by gel permeation chromatography using poly(ethylene glycol) standards.
[c] Determined by dynamic light scattering in serum-free Dulbecco's modified Eagle's Medium (DMEM). The parentheses indicate polydispersity index (PI).
[d] Measured in serum-free DMEM.